

Orcokinin Peptides in Developing and Adult Crustacean Stomatogastric Nervous Systems and Pericardial Organs

LINGJUN LI,^{1,2} STEFAN R. PULVER,² WAYNE P. KELLEY,¹
VATSALA THIRUMALAI,² JONATHAN V. SWEEDLER,¹ AND EVE MARDER^{2*}

¹Department of Chemistry and Beckman Institute, University of Illinois,
Urbana, Illinois 61801

²Volen Center and Biology Department, Brandeis University,
Waltham, Massachusetts 02454-9110

ABSTRACT

The orcokinins are a family of neuropeptides recently isolated from several crustacean species. We found orcokinin-like immunoreactivity in the stomatogastric nervous systems and pericardial organs of three decapod crustacean species, *Homarus americanus*, *Cancer borealis*, and *Panulirus interruptus*. The neuropil of the stomatogastric ganglion was stained in adults of all three species as well as in embryonic and larval *H. americanus*. In *H. americanus*, the somata giving rise to this projection were found in the inferior ventricular nerve. Matrix-assisted laser desorption/ionization mass spectrometry mass profiling and sequencing with postsource decay led to the identification of six different orcokinin family peptides, including those previously described in other decapods and two novel shorter peptides. Application of exogenous [Ala¹³]orcokinin to the stomatogastric ganglion of *H. americanus* resulted in changes in the pyloric rhythm. Specifically, the number of lateral pyloric (LP) neuron spikes/burst decreased, and the phase of firing of the pyloric neurons was altered. Together, these data indicate that the orcokinins are likely to function as modulators of the crustacean stomatogastric ganglion. *J. Comp. Neurol.* 444:227–244, 2002. © 2002 Wiley-Liss, Inc.

Indexing terms: MALDI-TOF mass spectrometry; neuromodulators; *Homarus americanus*; *Cancer borealis*; *Panulirus interruptus*; confocal microscopy

The crustacean stomatogastric nervous system contains the central pattern-generating networks that control rhythmic movements of the foregut (Harris-Warrick et al., 1992). One of the most remarkable features of this nervous system is the richness and diversity of its neuromodulatory control systems. Specifically, although the stomatogastric ganglion (STG) contains only 26–30 neurons, 18–20 different neuromodulators are found in neurons that project into the STG (Marder et al., 1995; Marder and Calabrese, 1996). Moreover, these and additional substances are also present in the hemolymph, as a consequence of their release by the pericardial organs and other neurosecretory structures (Christie et al., 1995b).

The orcokinins are a novel family of neuropeptides that were originally purified from the nervous system of the crayfish *Orconectes limosus* (Stangier et al., 1992) and measured by ELISA in various neural structures, including the STG, in several crustacean species (Bungart et al., 1994). Subsequently, different orcokinin analogues were isolated, and it is now evident that the orcokinins are a

family of closely related peptides (Bungart et al., 1995a,b; Dirksen et al., 2000; Yasuda-Kamatani and Yasuda, 2000).

Immunocytochemical localizations of the orcokinin family reveal cells and fibers that stain in the sixth abdominal ganglion of *O. limosus* and fibers throughout the gut. We (this paper) and Skiebe et al. (2002) have combined immunocytochemistry and matrix-assisted laser desorption/ionization (MALDI) time-of-flight mass spectrometry (TOF MS) to describe the presence and structure of the orcokinin peptides in the stomatogastric nervous systems and pericardial organs of several crustacean species.

*Correspondence to: Dr. Eve Marder, Volen Center, MS 013, Brandeis University, 415 South St., Waltham, MA 02454.
E-mail: marder@brandeis.edu

Received 17 July 2001; Revised 12 October 2001; Accepted 16 November 2001

Because the orcokinin antisera used for immunocytochemistry (Dirksen et al., 2000) do not distinguish among several structurally distinct peptide forms, biochemical characterization of the peptides in different tissues and species allows us to determine unambiguously which of the peptides are found in the stomatogastric nervous system of each crustacean studied.

Despite the extensive biochemical characterization of the orcokinins, relatively little is known of their physiological roles. To date, the bioactivity of the orcokinins has been demonstrated in the hindgut of the crayfish (Stangier et al., 1992; Bungart et al., 1995b; Dirksen et al., 2000), but no electrophysiological demonstrations of the effects of the orcokinins on the nervous system have been reported. The distribution of orcokinin-like immunoreactivity in the stomatogastric nervous system suggested that orcokinin family peptides could function as modulators of the stomatogastric nervous system motor patterns, motivating us to study the modulation of the pyloric rhythm of the stomatogastric nervous system in *Homarus americanus* by orcokinin.

Recent work has shown that the full complement of neuromodulators in the adult stomatogastric nervous system does not appear until the end of larval life. Instead, individual sensory and descending neurons that project into the STG acquire their full complement of neurotransmitters sequentially (Fénelon et al., 1998, 1999; Kilman et al., 1999; Le Feuvre et al., 2001). The timing of appearance of the orcokinins in development has not been previously studied. Therefore, one of the goals of this work was to determine the developmental timing of orcokinin appearance in the stomatogastric nervous system and pericardial organs of *H. americanus* and to compare these with the developmental appearance of the other major STG neuromodulators.

Previous work on the modulatory projections to the STG on related crustacean species has demonstrated significant differences in the distribution of modulators in the stomatogastric nervous system (Beltz et al., 1984; Mortin and Marder, 1991; Turrigiano and Selverston, 1991; Skiebe, 1999), including species differences in the cotransmitter complement of identified projection neurons (Meyrand et al., 2000). For this reason, here we also compared

the distribution of orcokinin family peptides in the adult nervous system of three species of crustaceans, *H. americanus*, *Cancer borealis*, and *Panulirus interruptus*. These will be further compared with the results for *Cherax destructor* obtained by Skiebe et al. (2002). Some of this work has been presented in abstract form (Li et al., 2001).

MATERIALS AND METHODS

Animals and dissection

Experiments were performed on embryonic, larval, juvenile [thorax length (TL) 1–2 cm], and adult *H. americanus*. Embryos, larvae, and juveniles were obtained from the lobster-rearing facility at the New England Aquarium (Boston, MA); adults were obtained from Commercial Lobster (Boston, MA). Experiments were also performed on adult *C. borealis* and *P. interruptus* (TL 6–8 cm). *C. borealis* and *P. interruptus* were obtained from Commercial Lobster and Tomlinson Commercial Fishery (San Diego, CA), respectively. Animals were kept in large tanks of circulating 10–14°C seawater. *H. americanus* embryos and larvae were staged according to Helluy and Beltz (1991).

In adult, older larval, and juvenile animals, the STG and nerves of the stomatogastric nervous system were dissected free of the stomach and pinned flat onto a Sylgard-lined petri dish, as is customary for STG preparations (Harris-Warrick et al., 1992). The pericardial organs (POs) in adults of all three species were dissected by removing the carapace covering the heart. The longitudinal body muscles, hyperdermis, and heart were then removed and pinned ventral side up in a Sylgard-lined petri dish. The PO nerves surrounding the heart were identified and removed. The dissection procedures for embryos and smaller larvae for the stomatogastric nervous system in *H. americanus* were carried out as previously described (Kilman et al., 1999). Briefly, the foregut was removed, split open along the midline, and pinned flat onto a small Sylgard cube.

The saline composition for *H. americanus* and *P. interruptus* was (in mM) NaCl, 479; KCl, 12.74; MgSO₄, 20; Na₂SO₄, 3.91; CaCl₂, 13.67; HEPES, 5; pH 7.45. For *C. borealis* the saline composition was (in mM) NaCl, 440; KCl, 11; MgCl₂, 26; CaCl₂, 13; Trizma base, 11; maleic acid, 5; pH 7.4–7.5.

Whole-mount immunocytochemistry

Tissues were processed for whole-mount immunocytochemistry following standard protocols for this system (Beltz and Kravitz, 1983). Tissues were fixed overnight at 4°C with one of two solutions. Embryonic and larval *H. americanus* preparations were fixed with 2% paraformaldehyde and 15% picric acid in 0.2 M sodium phosphate buffer, pH 7.3 (Stefanini et al., 1967). Juvenile *H. americanus*, *C. borealis*, and *P. interruptus* were fixed with 4% paraformaldehyde in 0.1 M sodium phosphate buffer, pH 7.4. In all species, the same structures were labeled with either Stefanini fixative or 4% paraformaldehyde (S.R.P., unpublished observations).

After fixation, preparations were washed five or six times for 1 hour per wash in 0.1 M sodium phosphate buffer, pH 7.4, containing 0.3% Triton X-100 and 0.1% sodium azide (PTA). The tissues were then incubated for approximately 12–24 hours in a polyclonal primary antiserum raised in rabbits against a thyroglobulin conjugate

Abbreviations

| | |
|-----------|--|
| CabTRPIa | <i>Cancer borealis</i> tachykinin-related peptide Ia |
| Co | commissures |
| CoG | commissural ganglion |
| dvn | dorsal ventricular nerve |
| dpon | dorsal posterior esophageal nerve |
| ion | inferior esophageal nerve |
| ivn | inferior ventricular nerve |
| IV neuron | inferior ventricular neuron |
| LP neuron | lateral pyloric neuron |
| lvn | lateral ventricular nerve |
| np | neuropil |
| OG | esophageal ganglion |
| on | esophageal nerve |
| PD neuron | pyloric dilator neuron |
| pdn | pyloric dilator nerve |
| PY neuron | pyloric neuron |
| pyn | pyloric nerve |
| PS | pyloric suppressor |
| som | somata |
| son | superior esophageal nerve |
| STG | stomatogastric ganglion |
| stn | stomatogastric nerve |

of [Asn¹³]orcokinin that cross reacts with others of the family of orcokinin peptides (Bungart et al., 1994; Dircksen et al., 2000). This antibody was a gift of Heinrich Dircksen (Bonn, Germany) and was used at a final dilution of 1:5,000. The primary antiserum was diluted in PTA plus 10% goat normal serum (GNS) to reduce nonspecific staining. Preparations were washed in PTA as described above and then incubated overnight in PTA plus 10% GNS along with anti-rabbit Alexafluor 488 (Molecular Probes, Eugene, OR) diluted 1:300–1:400. Finally, preparations were washed five or six times for 1 hour per wash in 0.1 M sodium phosphate buffer, pH 7.4. The tissues were mounted in 80% glycerol in 0.02 M sodium phosphate buffer, pH 7.4, on glass slides. All processing was carried out at 4°C.

Imaging

Preparations were viewed as whole mounts with a Bio-Rad MRC 600 laser scanning confocal microscope with a krypton/argon mixed gas laser or a Leica TCS spectral confocal microscope fitted with argon (458/488 nm) and krypton (568 nm) lasers. For imaging antibodies coupled to Alexafluor 488 on the Bio-Rad MRC 600, we used a standard BHS (exciter filter, 488 nm DF 10; dichroic reflector, 510 nm LP; emission filter, 515 nm LP) filter block. The z-axis spacing was 1–2 µm in embryos and larval *H. americanus*. In adult animals, the z-axis spacing was 3 µm except in the commissural ganglia (CoGs), which were sometimes sectioned at 4 or 5 µm intervals because of the large size of these ganglia. The resulting stacked images were compiled into maximum projections, then processed with Confocal Assistant (Bio-Rad) and Adobe Photoshop 5.5 (Adobe Systems, Mountain View, CA). Images were printed on a Codonics NP-1600 Printer (Codonics Inc., Middleburg Heights, OH).

Cellular sample preparation for MALDI-MS analysis

Small pieces of tissue samples or single neurons were dissected and prepared for MALDI-MS analysis. Physiological saline was replaced with an aqueous MALDI matrix solution, 10 mg/ml of 2,5-dihydroxybenzoic acid (DHB; ICN Pharmaceuticals, Costa Mesa, CA) to remove the extracellular salts associated with the tissue sample (Garden et al., 1996). Tungsten needles and fine forceps were used to dissect and transfer small pieces of tissue or single neurons onto a MALDI sample plate containing 0.5 µl of either regular aqueous DHB (10 mg/ml) matrix solution or concentrated DHB (50 mg/ml) in acetone:water (4:1) mixed solvent. The tissue samples on the plate were smashed before drying at ambient temperature, followed by MALDI-MS analysis.

Microbore RP-HPLC of homogenates

Peptides were extracted from four brains from *H. americanus*, nine brains from *C. borealis* and a single brain from *P. interruptus*. In addition, 12 POs from *H. americanus* and 13 POs from *P. interruptus* were individually extracted and pooled. The extraction of tissues was performed using acidified acetone (1:40:6 HCl:acetone:H₂O) as described previously (Floyd et al., 1999). Briefly, samples were homogenized in a microhomogenizer (Jencons Scientific Ltd.), and the supernatant was drawn off and centrifuged (Baxter Bioflux 15, McGraw Park, IL). This

process was repeated several times, after which an addition of H₂O was made to the resulting extract, which was then concentrated under a stream of nitrogen to approximately 300 µl. Separations were performed utilizing a microbore HPLC instrument (Magic 2002; Michrom BioResources, Auburn, CA). An aliquot of the extract was injected onto a reverse-phase C-18 column (Reliasil). Both 1.0 × 150 mm and 0.5 × 150 mm columns were utilized, each with 5 µm particle size and 30 nm pore size. The column was equilibrated with solvent A at a programmed temperature of 35°C. An aliquot of the aqueous extract was injected onto the column at a constant flow rate of 50 µl/minute and a gradient developed from 5% to 98% of solvent B in 34 minutes. Solvent A consisted of 2% acetonitrile (ACN), 98% H₂O, and 0.1% trifluoroacetic acid (TFA; v/v). Solvent B consisted of 95% ACN, 5% H₂O, and 0.1% TFA (v/v). Sample peaks were detected via absorbance at 214 and 280 nm wavelengths, and the eluent was collected by a small-volume fraction collection system (Gilson FC 203B, Middletown, WI). To identify peptides of interest, each fraction was screened using MALDI-MS; approximately 0.25 µl of each fraction was deposited on a MALDI-MS sample plate, followed by the same volume of an α-cyano-4-hydroxycinnamic acid matrix (10 mg/ml in 6:3:1 ACN:H₂O:3% TFA; Aldrich, Milwaukee, WI). Thus more than 95% of each fraction was available for further assays.

MALDI-MS

MALDI is a soft ionization method that vaporizes and generates ions of analyte molecules without fragmenting them by incorporating the analyte into an excess of a matrix. The matrix is typically a small organic compound with absorbance at a wavelength of the laser employed. MALDI mass spectra were obtained using a Voyager DE STR (PE Biosystems, Framingham, MA) time-of-flight mass spectrometer equipped with delayed ion extraction. A pulsed nitrogen laser (337 nm) was used as the desorption/ionization source, and positive-ion mass spectra were acquired using both linear and reflectron modes. Each representative mass spectrum shown is the smoothed average of 128–256 laser pulses. Mass calibration was performed externally using a mixture of synthetic peptide standards (PE Biosystems). Mass accuracy was typically better than 0.01%. Because the signal intensity of MALDI spectra depends on the incorporation of the peptides into matrix crystals, it is difficult to relate peak height with the quantity of analyte present. Thus, MALDI is used primarily as a qualitative technique, and representative spectra of multiple replicates (n > 3) are shown in the current study.

Postsource decay (PSD) analysis

Semipurified microbore LC fractions containing the peptide of interest or 2 pmol of synthetic peptide standard were subjected to PSD analysis. The peptide standard [Ala¹³]orcokinin was synthesized by the Protein Sciences Facility (Biotechnology Center, University of Illinois). The total acceleration voltage was 20 kV, and a delay time of 75 nsec was used. By the use of timed ion selector, different precursor ions were selected from a mixture of peptides and subjected to fragmentation. Under these experimental conditions, the mass accuracy of the precursor ion was within 30 ppm, and the average error on the mass assignment of the PSD ions was better than 0.3 Da. Spec-

tra were obtained by accumulating data from 100–256 laser shots. To obtain complete PSD spectra, a series of reflectron TOF spectral segments was acquired, each optimized to focus fragment ions within different m/z ranges (Spengler, 1997). Each segment was stitched together using the Biospectrometry Workstation software to generate a composite PSD spectrum.

Electrophysiology

The entire stomatogastric nervous system was dissected. The STG was desheathed and Vaseline wells were made on the motor nerves for extracellular recordings. The preparations were continuously superfused with chilled saline (9–12°C). Intracellular recordings were made with glass microelectrodes filled with 0.6 M K_2SO_4 and 20 mM KCl, with typical resistances of 20–30 M Ω . Lateral pyloric (LP), pyloric (PY), and pyloric dilator (PD) neurons were identified on the basis of the motor nerves into which their axons project. The STG was left attached to the CoGs and the esophageal ganglion (OG) via the stomatogastric nerve (stn). Physiological saline containing 2×10^{-6} M [Ala^{13}]orcokinin was superfused over the entire preparation. Data were acquired using an Axoclamp 2A amplifier and a Digidata 1200 data acquisition board (Axon Instruments, Foster City, CA). Bursts and spikes were extracted using in-house software from the intracellular traces of the LP, PY, and PD neurons. From these data, the burst frequency, the number of spikes per burst, and the burst durations were calculated for each neuron type. Data obtained in normal saline were compared with those in orcokinin using paired t -tests in Microsoft Excel.

RESULTS

The stomatogastric nervous system

The stomatogastric nervous system consists of the single STG with about 30 neurons, the paired CoGs, the single OG, and their connecting nerves (Fig. 1). This general organization is the same in the three species studied—*H. americanus*, *C. borealis*, and *P. interruptus*—with the exception that the stn is shortened in the crab preparations relative to what is seen in the lobsters.

Previous work has demonstrated in *H. gammarus* that the complete stomatogastric nervous system is present before 50% of embryonic development (E50) and that as early as E50 neurogenesis in the STG is complete (Fénelon et al., 1998). More recently, LeFeuvre et al. (2001) suggested that most of the fibers projecting to the STG from the CoGs and the OG are also present by midembryonic life. Nonetheless, the gross anatomical features of the stomatogastric nervous system change during embryonic and larval life, as the nerves elongate and ganglia change shape. Despite the fact that the gross anatomical features of the stomatogastric nervous system are fully formed early in embryonic life, many of the neuromodulators found in projections to the STG from more anterior structures do not appear until later in development (Fénelon et al., 1998, 1999; Kilman et al., 1999; Le Feuvre et al., 2001), so we have studied orcokinin immunoreactivity at different developmental stages.

Orcokinin labeling in the STG in embryonic, larval, and adult *H. americanus*

Figure 2 shows whole mounts of STGs at different developmental stages labeled with the orcokinin antibody.

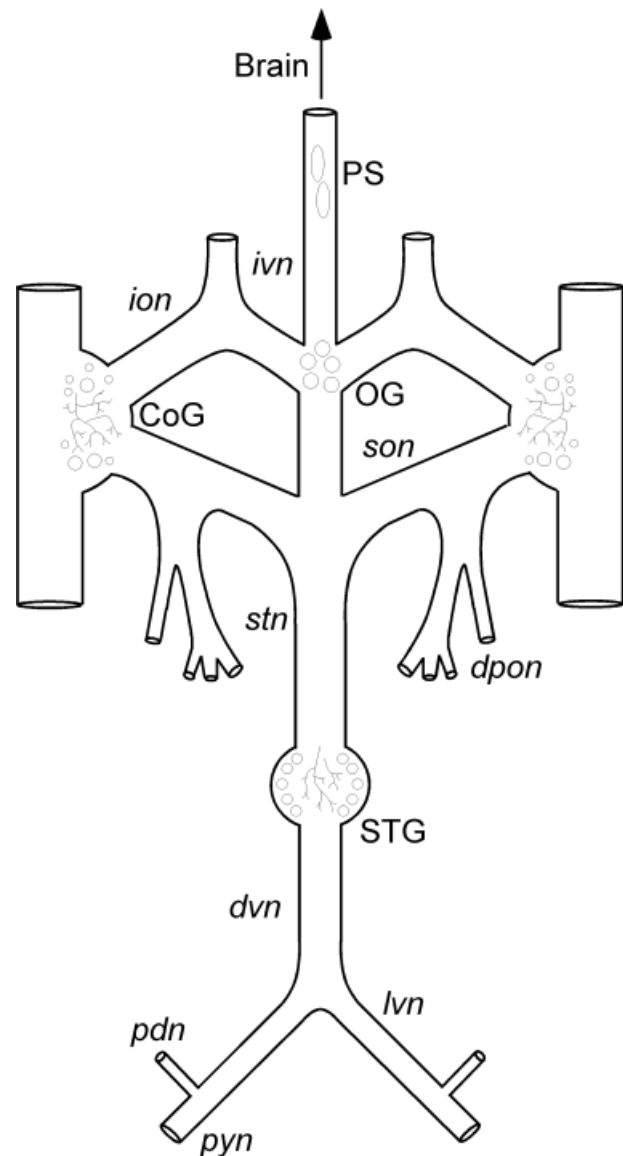


Fig. 1. Schematic diagram of the stomatogastric nervous system. The single STG receives modulatory descending inputs from neurons in the OG and the paired CoGs via the single stn. The ivn contains the somata of the PS neurons and connects the stomatogastric nervous system to the brain. The ion, son, dvn, pdn, pyn, and dpon are also indicated. Ganglion size and nerve width are not to scale.

Figure 2A shows that the neuropil of the STG of an E57 embryo was already densely immunoreactive for orcokinin. The single input nerve to the STG, the stn, showed at least one stained fiber, but none of the somata was labeled, and there were no labeled fibers in the posterior motor nerves. Similar staining patterns were seen in six embryos from E57 to E90. The same essential features of the orcokinin labeling were seen at later developmental times, except at later stages two stained fibers were visible in the stn. In a small number of preparations (1 of 6 embryos, 2 of 14 larvae, 0 of 4 juveniles, and 1 of 5 adults), one or two lightly labeled fibers were seen in the dorsal ventricular nerve (dvn). Figure 2B shows the STG from an

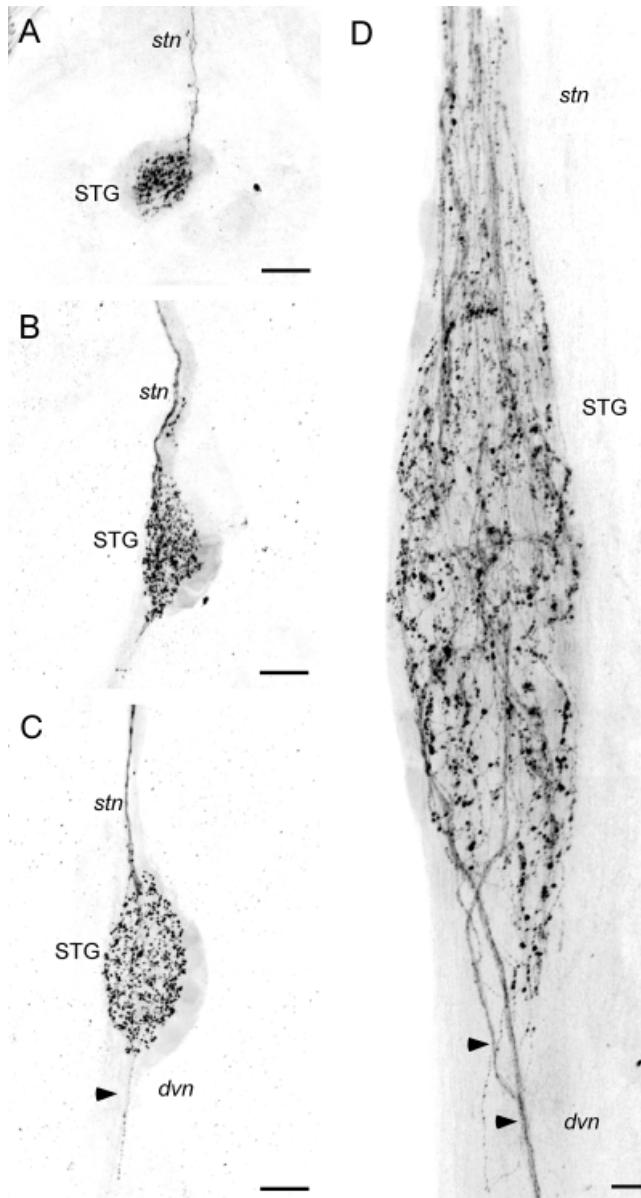


Fig. 2. Orcokinin-like immunoreactivity in the STG of the lobster *H. americanus* through development. All images are maximum projections of whole mounts. **A:** E57. **B:** LII. **C:** LIV. **D:** Adult. Arrows show stained fibers trailing into the dvn. Scale bars = 50 μm .

LII animal. The neuropil and stn were densely labeled, but no STG somata or motor nerves were stained ($n = 14$ larvae). Figure 2C,D shows STGs from an LIV and an adult animal. These images show varicosities and fibers in the neuropil and lightly stained fibers in the dvn, but no stained somata.

Orcokinin labeling in the OG, CoGs, and ivn of *H. americanus* through development

Orcokinin-like immunoreactivity was present in two cell bodies in the OG as early as E50 of embryonic development. Figure 3A shows a whole-mount preparation taken

at E70. Interestingly, at this very early stage, the somata of these neurons are already quite large ($\sim 25 \mu\text{m}$). Even more heavily stained at this time were the two PS neurons in the inferior ventricular nerve (ivn; Fig. 3A), which in embryos can be traced into the OG. In embryos, two orcokinin-stained fibers were seen in the stn and one stained fiber in the superior esophageal nerve (son) and inferior esophageal nerve (ion).

Figure 3B shows the pair of stained OG neurons and the PS neurons in an LIII preparation. Even at this time, these pairs of neurons are quite prominent, in comparison with the other structures present. In LIII animals the PS neurons can be traced into the OG and out the ion. Additionally, there are two fibers that project into the stn down to the STG. When the animals reach juvenile stages (Fig. 3C), the preparations take on adult proportions. In this particular preparation, the PS neurons were heavily stained, and the pair of OG somata was only very lightly stained. Figure 3C shows the fiber ribbons from the PS neurons as they project into the ion and the more punctate staining seen in the PS fibers as they project down the esophageal nerve (on) and into the son and the stn. These OG cells were also visible in all larval ($n = 14$) and juvenile ($n = 4$) preparations, with variable intensity of staining (Fig. 3B,C).

Orcokinin-like immunoreactivity was also present in CoG neuropil and multiple CoG somata (Figs. 3A,B, 4). Figure 4A shows a high-magnification view of the CoG from an E70 embryo. Punctate neuropil staining and fibers in the commissures are clearly evident. Four or five somata were clearly stained at this time. Also visible in Figures 3A and 4A are somata in the neighboring brain regions. Figure 4B shows a CoG from an LIII animal. Somata (six to eight clearly stained in each ganglion), neuropil, and fibers in the CoG were clearly evident. Figure 4C shows a CoG from a juvenile animal. Clearly visible are three or four large somata ($\sim 50 \mu\text{m}$), five or six medium-sized somata ($\sim 30\text{--}40 \mu\text{m}$), and a larger number (15–20) of more lightly stained smaller somata. Fibers in the commissures are clearly visible, as are fibers in both the ion and the son.

We counted the number of stained fibers in each of the nerves shown in Figure 1. The stn in adults has four clearly stained orcokinin fibers, each son has three or four fibers, each ion has two or three fibers, and the ivn has four fibers below the level of the PS neurons and two fibers above the level of the PS neurons.

Figure 5 is a summary of the distribution of orcokinin-like immunoreactivity at different developmental stages in *H. americanus*. The numbers of stained somata and fibers are indicated where appropriate. Comparison of these schematics shows that, although the main features of the projections from the PS cells are present quite early, the full complement of orcokinin staining CoG cells and fibers in the connecting nerves does not become evident until much later in development.

Orcokinin-like immunoreactivity in the stomatogastric nervous system of the crab *C. borealis*

The distribution of orcokinin-like immunoreactivity was somewhat different in *C. borealis* than that in *H. americanus*. Figure 6A shows the orcokinin-like immunoreactivity in *C. borealis* STG. There are densely stained fibers

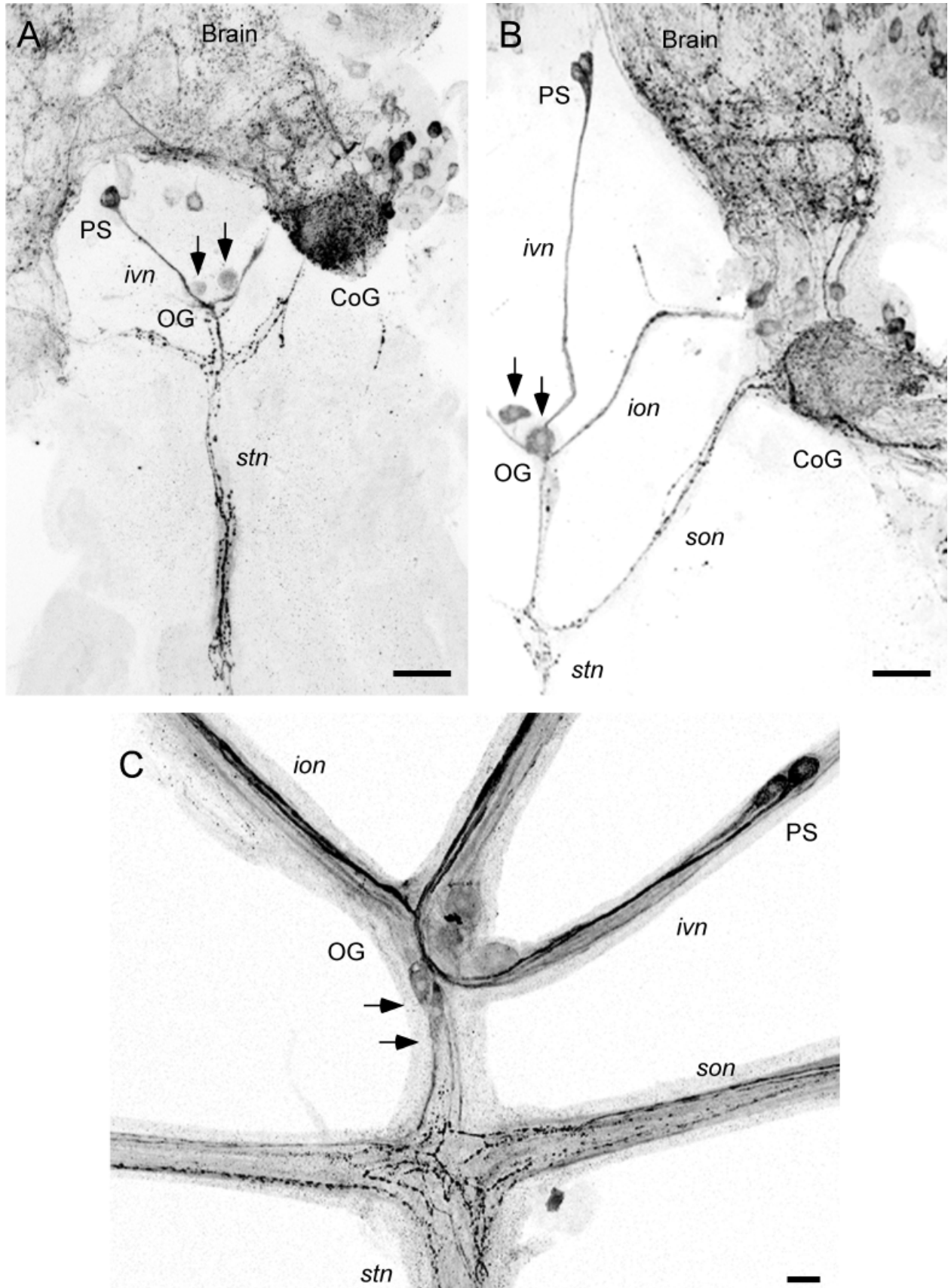


Fig. 3. Orcokinin-like immunoreactivity in the OGs of *H. americanus* during development. **A:** E70. **B:** LIII. **C:** Juvenile (thorax length 1.8 cm). Arrows indicate the stained OG somata. Scale bars = 50 μm.

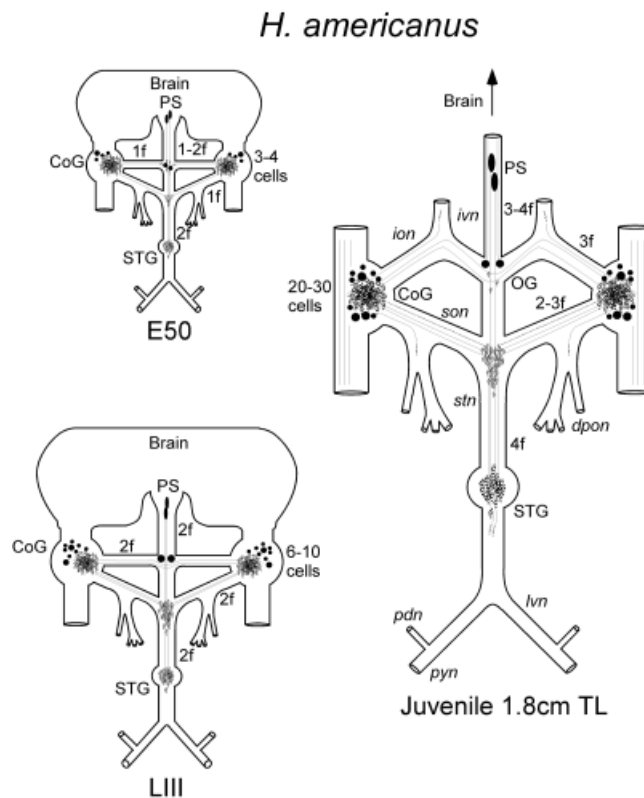
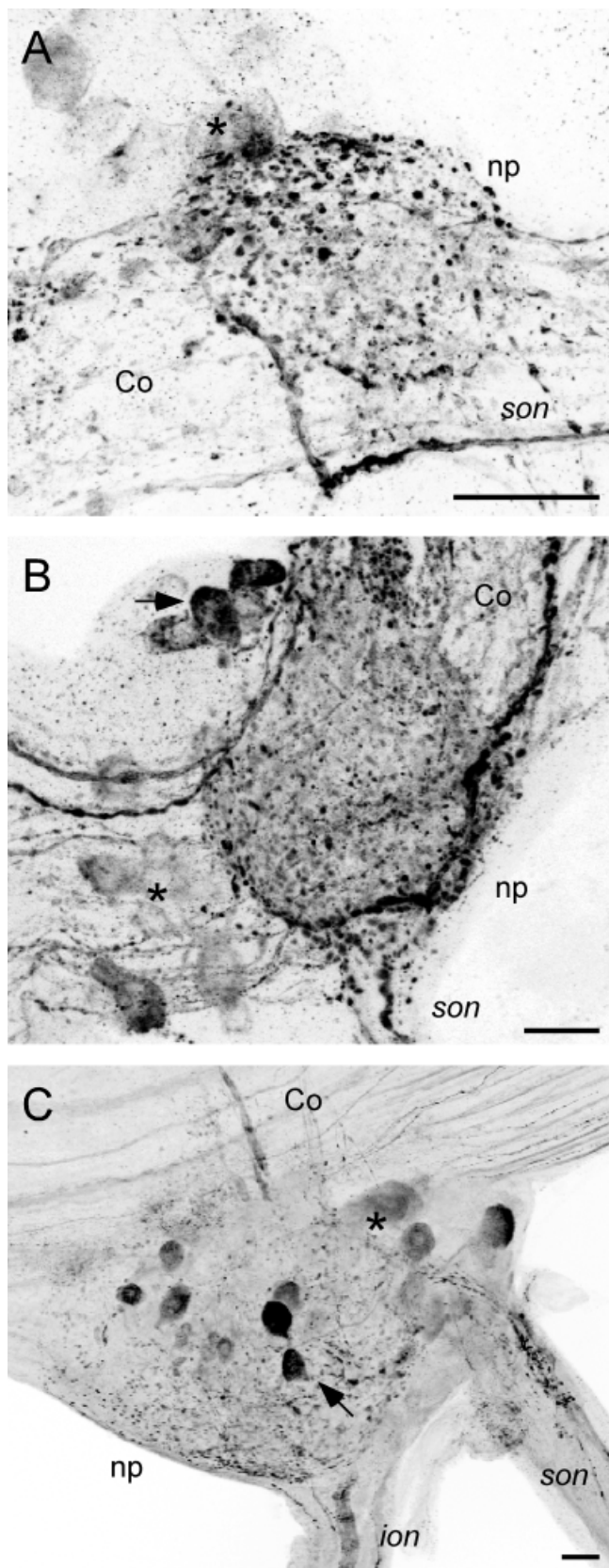


Fig. 5. Summary of the orcokinin-like distribution at three developmental stages in *H. americanus*. The number of fibers (f) is indicated next to each nerve.

in the stn and heavily stained neuropil processes. Additionally, there are two faintly stained STG somata (two faint somata were seen in 4 of 7 preparations). Figure 6B shows the junction between the sons and the stn. This junction shows fibers running in each son and the stn. Additionally, there is neuropil-like varicose staining at the junction, similar to what is seen there for other neuropeptides (Kilman, 1998; Skiebe and Ganeshina, 2000). Figure 6C shows two densely stained OG somata ($n = 7$ preparations) that project into the ivn. The CoG (Fig. 7A) shows punctate neuropil, 3 large ($\sim 100 \mu\text{m}$) weakly stained somata, and 15–20 smaller, variably stained somata. The commissures (Fig. 7A) show a large number of stained fibers. A novel feature of the staining in *C. borealis* was the large number of fibers in the dorsal posterior esophageal nerve (dpon), a branch off the son (Fig. 7B,C). The dpon carries innervation to and from the cardiac sac wall and muscles. Partway down the dpon, three bipolar somata were found, two of which are shown in Figure 7D. Figure 7B shows that these bipolar neurons account for only a small proportion of the stained fibers in the dpon. Overall, there were considerably more stained fibers in

Fig. 4. Orcokinin-like immunoreactivity through development in the CoGs of *H. americanus*. **A:** E70. **B:** LIII. **C:** Juvenile. Asterisks indicate groups of lightly stained somata. Arrows show darkly stained somata. Scale bars = $50 \mu\text{m}$.

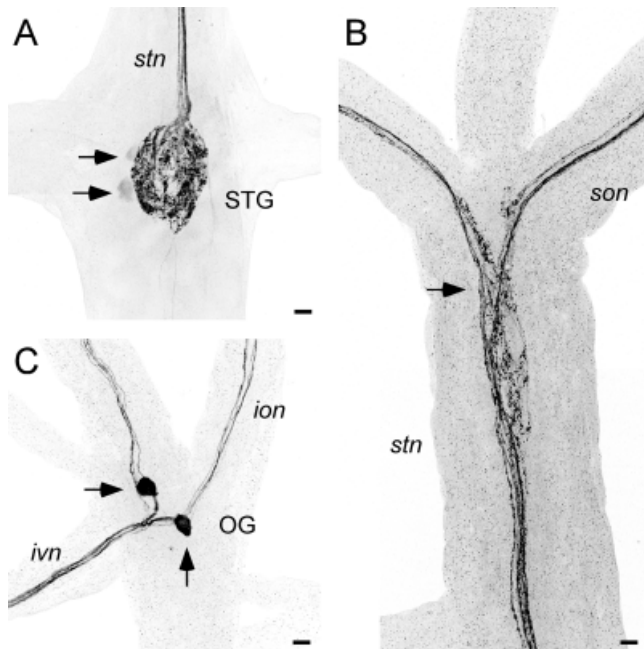


Fig. 6. Orcokinin-like immunoreactivity in STG and OG of adult *C. borealis*. **A:** STG and stn. Note the two faintly stained STG somata (arrows). **B:** Montage (of three micrographs) of the junction of the sons and stn shows varicose ramifications (arrow). **C:** OG with two darkly stained somata (arrows) projecting up into the ivn. Scale bars = 50 μm .

C. borealis than in *H. americanus*. In *C. borealis* there were six to ten stained fibers in the stn, five or six stained fibers in the son, three or four stained fibers in the ion, and three or four stained fibers in the ivn.

Distribution of orcokinin-like immunoreactivity in the stomatogastric nervous system of *P. interruptus*

The distribution of orcokinin-like immunoreactivity in *P. interruptus* was less extensive than in the other species ($n = 5$, three adults and two juveniles). Figure 8A shows orcokinin staining in the STG of a juvenile animal. The stn descending projection contains a tightly packed bundle of four to six small-diameter fibers that enter the STG and ramify through the neuropil. No somata or posterior motor nerves were stained. A novel feature of the *P. interruptus* pattern was the presence of two small ($\sim 20 \mu\text{m}$) somata at the junction of the sons and stn. Orcokinin-staining neuropil was also seen in the stn close to the junction with the sons (Fig. 8B). Figure 8C shows the presence of two somata in the OG that project axons up the ivn, toward the brain ($n = 5$). The distribution of immunoreactivity in the CoGs of *P. interruptus* is less extensive than seen in the other animals and is shown in the summary diagram in Figure 9, along with the summary of the distribution of immunoreactivity in *C. borealis*.

Orcokinin staining in the pericardial organs

The crustacean POs are one of the major neurosecretory structures in the animal, releasing numerous hormones that regulate a variety of physiological processes (Cooke

and Sullivan, 1982; Keller, 1992; Dirksen, 1997). Figure 10 shows that dense orcokinin-like immunoreactivity is present in fibers and varicosities in the POs of all three species studied here ($n = 5$ *H. americanus*, $n = 3$ *C. borealis*, $n = 5$ *P. interruptus*).

MALDI analysis of orcokinin family peptides

For the preceding sections of this paper, we used an antibody to map the distribution of orcokinin-like neuropeptides. For this section we use biochemical techniques to determine the identity of the peptides that give rise to the orcokinin-like immunoreactivity. MALDI-MS is a powerful technique for the simultaneous detection of multiple peptides present at significant levels in biological tissues or even single cells with minimal sample preparation (Jiménez et al., 1994; Garden et al., 1996, 1998; Martin et al., 1999). Since the original orcokinin was isolated from the crayfish *Orconectes limosus* (Stangier et al., 1992), analogues of orcokinin have been identified in tissues from the shore crab *Carcinus maenas* (Bungart et al., 1995a). The sequence of the original orcokinin is Asn-Phe-Asp-Glu-Ile-Asp-Arg-Ser-Gly-Phe-Gly-Phe-Asn ([Asn¹³]), and the three analogues of orcokinin differ in only one amino acid residue and so are named [Ser⁹]-, [Ala¹³]-, and [Val¹³]orcokinin (Bungart et al., 1995a).

We identified a total of six orcokinin-related peptides with MALDI-MS in *C. borealis*, *H. americanus*, and *P. interruptus* based on molecular weight measurements and the known peptide sequences from *O. limosus* and *C. maenas*. Some of these peptides are unique to one species, and others are common to all three species (Table 1).

Because the immunocytochemistry studies showed intense orcokinin staining in POs, to verify the peptide identity and determine the actual form(s) of the orcokinins present in this neurosecretory tissue that contribute to the orcokinin-like immunoreactivity seen in the POs, MALDI-MS peptide profiling of PO tissue from the three species was performed. Figure 11 shows a representative MALDI mass spectrum of PO tissue from *H. americanus*. Five forms of orcokinins were present, including [Asn¹³]orcokinin, its two C-terminally truncated forms, orcokinin[1–11] and orcokinin[1–12], and [Ala¹³]- and [Val¹³]orcokinins. MALDI-MS analysis of PO tissue extract from the crab *C. borealis* revealed the presence of [Ala¹³]-, [Val¹³]-, and [Ser⁹]orcokinins. PO tissue extract from *P. interruptus* contained the [Asn¹³]- and [Val¹³]orcokinins. Although molecular weight information is crucial for peptide identification, unambiguous identification is often achieved via mass spectrometric sequencing techniques. Therefore, we performed PSD (Spengler, 1997; Li et al., 1999) analysis of several orcokinin-containing LC fractions obtained from brain extracts to confirm these assignments. Figure 12 shows a representative PSD fragmentation ion spectrum of the precursor ion at m/z 1,517.6 and the peptide sequence analysis from *H. americanus* brain extract LC fraction. To use the established nomenclature, cleavage of an amide bond produces b-type ions (charge is retained at the N-terminus) and y-type ions (charge is retained at the C-terminus; Siuzdak, 1996). The sequence-specific fragment ions can thus be assigned as shown in Figure 12. By using the MS-Product database developed by the UCSF Mass Spectrometry Facility (<http://prospector.ucsf.edu>), with the entered orcokinin peptide sequence, fragment ions resulting from PSD processes were calculated by the software. The fragment ions

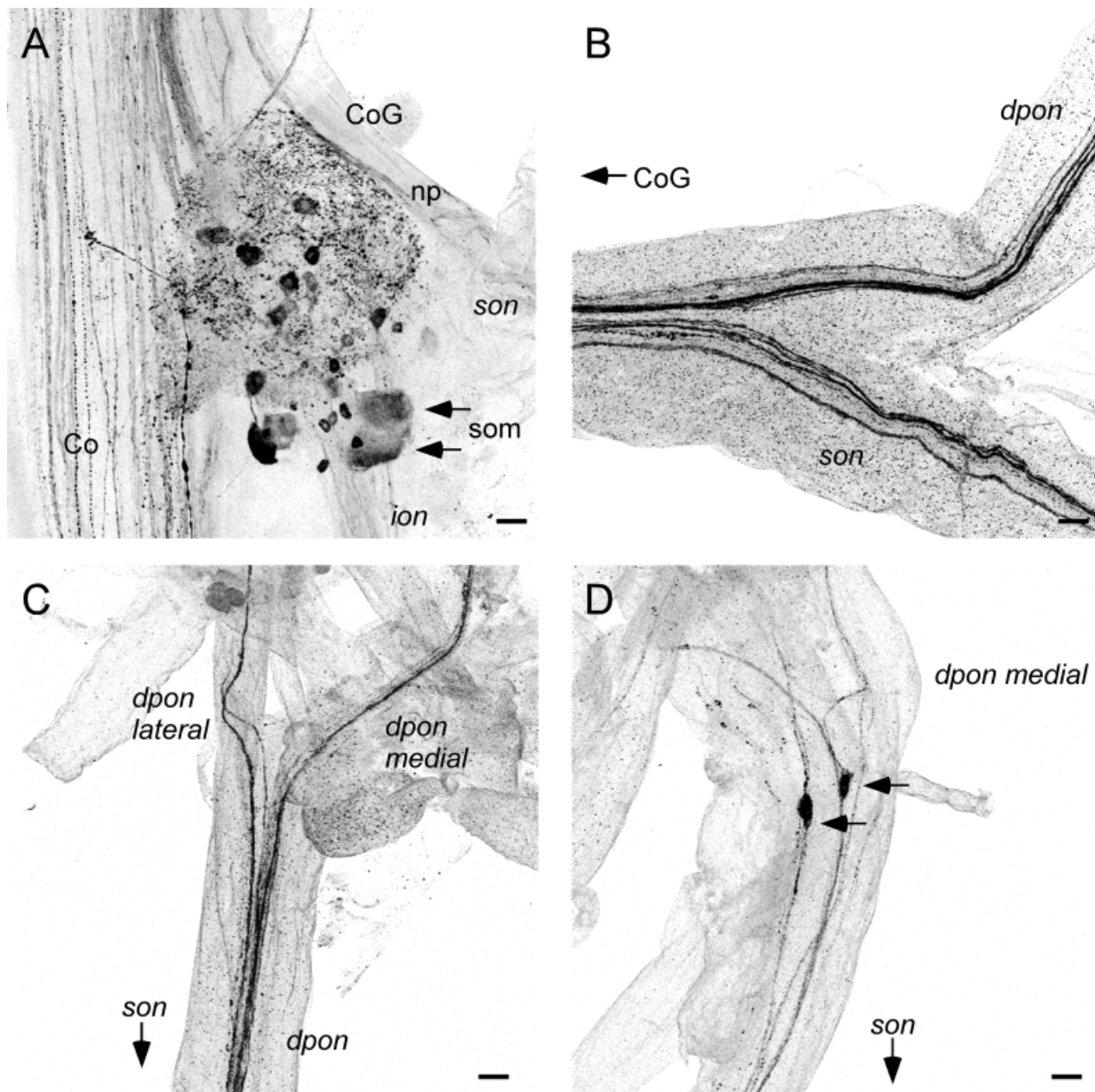


Fig. 7. Orcokinin staining in the CoGs and nerves of adult *C. borealis*. **A:** CoG. Arrows indicate two large, weakly stained somata. **B:** Branch of the dpon off of the son. **C:** Stained fibers splitting into different branches of the dpon. **D:** Two bipolar somata (arrows) in the medial branch of the dpon. Scale bars = 50 μm .

detected in the obtained PSD spectra match well with the predicted fragment pattern, which further confirms the identity of $[\text{Asn}^{13}]$ orcokinin.

Putative $[\text{Ala}^{13}]$ orcokinin (m/z 1,474.7) was present in brain extracts from *C. borealis*, *H. americanus*, and *P. interruptus* and was often the most intense peak in *C. borealis* tissue samples. Figure 13 shows the peptide sequence of $[\text{Ala}^{13}]$ orcokinin (Fig. 13A) and PSD spectra obtained from the putative $[\text{Ala}^{13}]$ orcokinin containing LC fraction from *C. borealis* brain extract (Fig. 13B, upper

trace) and the synthetic $[\text{Ala}^{13}]$ orcokinin standard (Fig. 13B, lower trace). The almost identical fragmentation pattern observed between the synthetic and the putative $[\text{Ala}^{13}]$ orcokinin PSD spectra confirms the identity of $[\text{Ala}^{13}]$ orcokinin in the brain extract. In fact, the extensive fragmentation obtained from the precursor ion at m/z 1,474.6 in the brain extract allowed complete de novo sequencing of the peptide. The immonium ions observed in the low-mass region of the spectrum (as highlighted in Fig. 13, inset) indicate the presence of amino acids, includ-

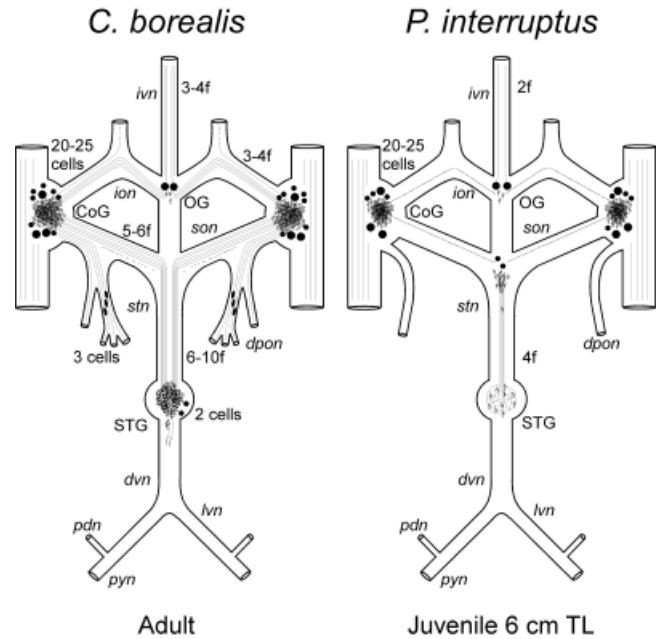
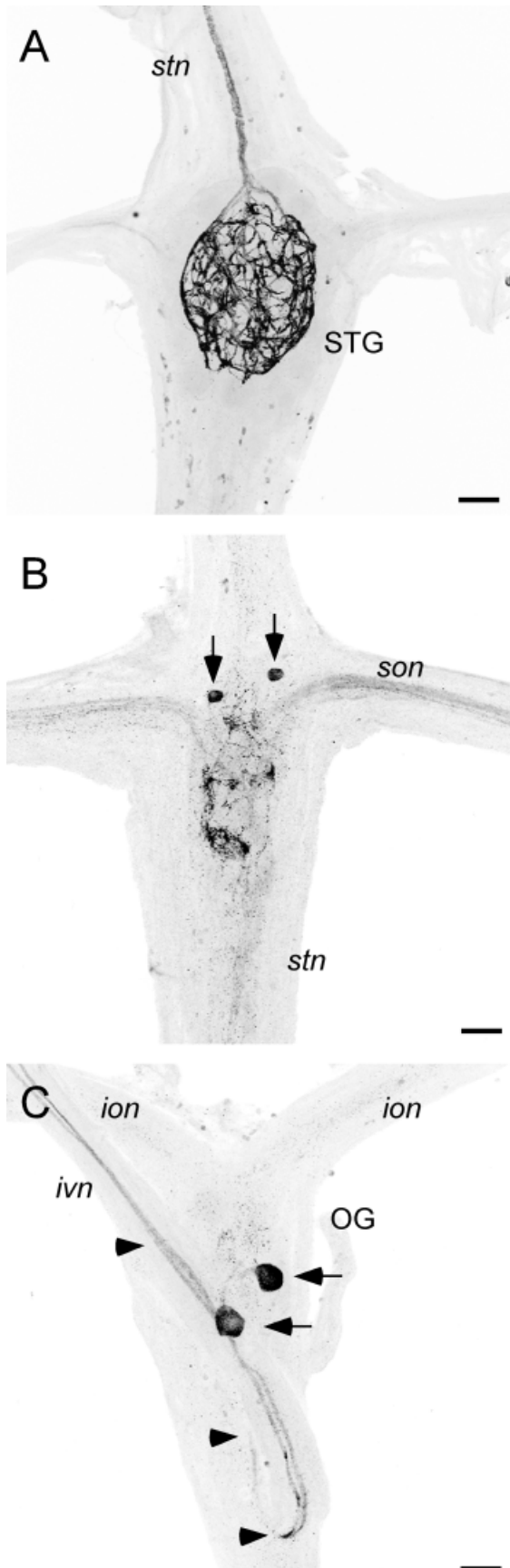


Fig. 9. Summary diagrams of the distribution of orckinin-like immunoreactivity in the stomatogastric nervous system of *C. borealis* and juvenile (6 cm TL) *P. interruptus*.

ing Ala (44 Da), Arg (129, 70, 87, 112 Da), Ile (86 Da), Asn (87 Da), Asp (88 Da), Glu (102 Da), and Phe (120 Da) and the absence of His (110 Da). Mass signal pairs ($m_b + m_y = m_{\text{precursor}} + 1$) at m/z 115.1/1,361.5, 262.3/1,214.3, 377.4/1,099.2, 506.5/970.0, 619.6/856.9, 734.7/741.8, 890.9/585.6, 978.0/498.5, 1035.1/441.5, 1182.2/294.3, 1239.3/237.3, and 1386.5/90.1 were assigned as paired b-type and y-type ions (see Fig. 13A). The b-type ions were determined based on the detection of their corresponding a-type ions (loss of CO, yielding a 28 Da lower mass ion). The amino acid sequence of the putative [Ala¹³]orckinin peak was deduced by using the mass difference between consecutive b- or y-type ions. The sequence was determined to be Asn-Phe-Asp-Glu-Ile/Leu-Asp-Arg-Ser-Gly-Phe-Gly-Phe-Ala, where the Ile and Leu could not be distinguished because of the identical mass of both residues. However, the 100% identity to the known sequence strongly suggests an Ile instead of Leu. Three other orckinin peptides were confirmed similarly (data not shown). Thus, by using a MALDI-based sequencing approach, all of the newly identified orckinin peptides have been confirmed.

After confirming all of the identified orckinin peptides, a MALDI-MS survey of the distribution of various forms of orckinins in different tissues from three crustacean species was conducted (Table 1). As noted, some of the orckinin forms are unique to one species, and others are

Fig. 8. Orckinin-like immunoreactivity in the stomatogastric nervous system of *P. interruptus*. **A**: STG. **B**: Junction of the stn and sons. Arrows indicate two small stained somata. **C**: OG. Arrowheads indicate the path of the two stained fibers in the ivn that project from the stained OG somata. The ivn is folded over the top of the left ion. Scale bars = 50 μm .

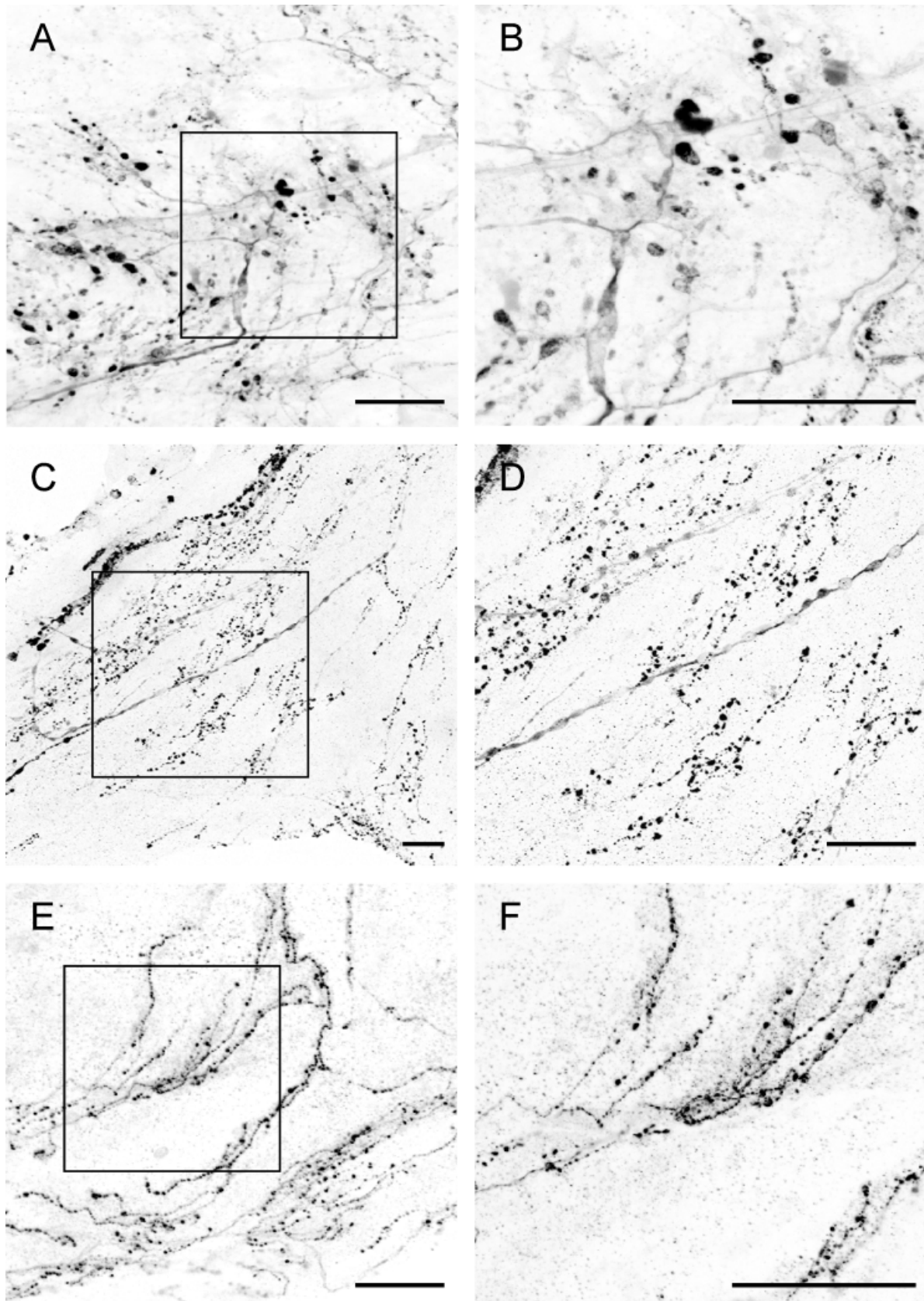


Fig. 10. Orcokinin-like immunoreactivity in the pericardial organs of *H. americanus* and *C. borealis* and the pericardial plexus of *P. interruptus*. **A:** Pericardial organ of adult *H. americanus*. **B:** High-magnification view of the box shown in A. **C:** Pericardial organ of

adult *C. borealis*. **D:** High-magnification view of the box shown in C. **E:** Pericardial plexus from adult *P. interruptus*. **F:** High-magnification view of the box shown in E. Scale bars = 50 μm .

TABLE 1. Orcokinin Distribution in Crustacean Species Revealed by MALDI-MS¹

| Sample ID | Orcokinin[1–11] 1,256.55 | Orcokinin[1–12] 1,403.63 | [Ala ¹³]orcokinin 1,474.65 | [Val ¹³]orcokinin 1,502.68 | [Asn ¹³]orcokinin 1,517.66 | [Ser ⁹]orcokinin 1,547.7 |
|---|-----------------------------|-----------------------------|---|---|---|---|
| <i>Homarus americanus</i> (adult) | | | | | | |
| STG | × | × | × | × | × | |
| CoG | × | × | × | × | × | |
| OG | × | × | × | × | × | |
| PO | × | × | × | × | × | |
| brain | × | × | × | × | × | |
| PS/IV | | | × | × | × | |
| ivn | | | × | × | × | |
| dpon | × | × | × | × | × | |
| son | | × | × | × | × | |
| dvn | × | | | × | | |
| ion | | | × | × | | |
| <i>Homarus americanus</i> (developmental) | | | | | | |
| STG | | | Embryo, LI, LII, LIII, LIV | Embryo, LI, LII, LIII, LIV | Embryo, LI, LIII, LIV | |
| CoG | | | LI, LII, LIII | LI, LII | LI, LIII | |
| <i>Cancer borealis</i> | | | | | | |
| STG | × | × | × | × | | × |
| CoG | × | × | × | × | | × |
| PO | | | × | × | | × |
| brain | × | × | × | × | | × |
| ivn | × | × | × | × | | × |
| <i>Panulirus interruptus</i> | | | | | | |
| STG | × | × | × | × | × | |
| CoG | × | × | × | × | × | |
| OG | × | × | × | × | × | |
| brain | × | × | × | × | × | |
| PO | | | | × | × | |
| ivn | × | × | × | × | × | |
| son | | | × | × | × | |
| ion | | × | × | × | × | |

¹Note: × indicates peptide present in the tissue examined. CoG, commissural ganglion; dvn, dorsal ventricular nerve; dpon, dorsal posterior esophageal nerve; ion, inferior esophageal nerve, IV, inferior ventricular neuron; ivn, inferior ventricular nerve; OG, esophageal ganglion; PO, pericardial organ; PS, pyloric suppressor; son, superior esophageal nerve; STG, stomatogastric ganglion; stn, stomatogastric nerve.

present in all three species. For example, [Ser⁹]orcokinin was present only in *C. borealis*, whereas [Ala¹³]- and [Val¹³]orcokinins were detected in all three species. Figure 14 shows representative MALDI mass spectra obtained from pieces of the STG from *H. americanus* and *C. borealis*. [Ser⁹]orcokinin was seen only in *C. borealis*, and [Asn¹³]orcokinin was detected only in *H. americanus*. However, [Ala¹³]- and [Val¹³]orcokinins and two C-terminally truncated orcokinins were detected in both species. Furthermore, MALDI mass profiling of CoG, STG, PO, and brain tissue in *C. borealis* also revealed the presence of a mass peak at m/z 1,554.7, which may correspond to another variant of orcokinin, [Thr⁸-His¹³]orcokinin, originally isolated from the crayfish *P. clarkii* (Yasuda-Kamatani and Yasuda, 2000). Because of the relatively low intensity of the signal, PSD fragmentation analysis was not attempted. Thus, the assignment of this peak as [Thr⁸-His¹³]orcokinin remains tentative.

Single-cell MALDI was attempted from several identified neurons from *H. americanus*. As shown in Table 1, direct MALDI assay of single PS neurons ($n = 2$, three replicates for each cell) from *H. americanus* revealed the presence of three forms of orcokinins, including [Ala¹³]-, [Val¹³]-, and [Asn¹³]orcokinins, corresponding to the intense orcokinin-like staining observed in this pair of neurons in the animal by immunocytochemistry.

Orcokinin-like immunoreactivity was present in the STG and other regions of the nervous system in *H. americanus* quite early in development. We were curious whether there was a developmental regulation of the form of orcokinin expressed. Therefore, we analyzed tissues from the embryo and larval developmental stages (Table 1). STGs from the embryo and early larvae showed all three orcokinins found in the adult STG, [Ala¹³]-, [Asn¹³]-, and [Val¹³]orcokinin.

Electrophysiology

In previous bioassays, several orcokinin forms were biologically active (Bungart et al., 1995b). As a first step in determining the possible physiological roles of the orcokinins as potential modulators of the STG, we synthesized [Ala¹³]orcokinin for use in electrophysiological studies. We chose [Ala¹³]orcokinin because it is present in all three species studied and is often a prominent peak in the MALDI spectrum. Therefore, this peptide appeared to be a good candidate for a physiologically active orcokinin.

The pyloric rhythm of the STG consists of repeating sequences of activity in the LP, PY, and PD neurons (Fig. 15A). When [Ala¹³]orcokinin was applied in the bath, this pattern of activity changed. Specifically, the number of LP neuron spikes/burst decreased from 10 ± 1.7 to 5.5 ± 1.8 ($n = 5$, $P < 0.05$). This was accompanied by a decrease in the duration of the LP burst from 470 ± 5 to 238 ± 6 msec ($n = 5$, $P < 0.05$). The PY neurons depolarized slightly; consequently, the amplitude of the PY membrane potential oscillations decreased in the presence of [Ala¹³]orcokinin. Additionally, in all five preparations, there was a modest increase in burst frequency with the application of [Ala¹³]orcokinin.

Figure 15B shows the effect of [Ala¹³]orcokinin on the phase relationships of the pyloric network neurons. These phase plots show the relative timing of the neurons' discharge patterns when burst frequency is normalized. The PD neurons' duty cycles (fraction of the burst period for which the neuron was active) were unaffected by [Ala¹³]orcokinin. The LP neuron burst was terminated earlier in orcokinin. Specifically, the LP off phase was 0.8 ± 0.02 in normal saline and 0.63 ± 0.04 in orcokinin ($P < 0.01$; $n = 5$, paired t -test). The LP neuron duty cycle was shortened from 0.28 ± 0.03 in control saline to $0.16 \pm$

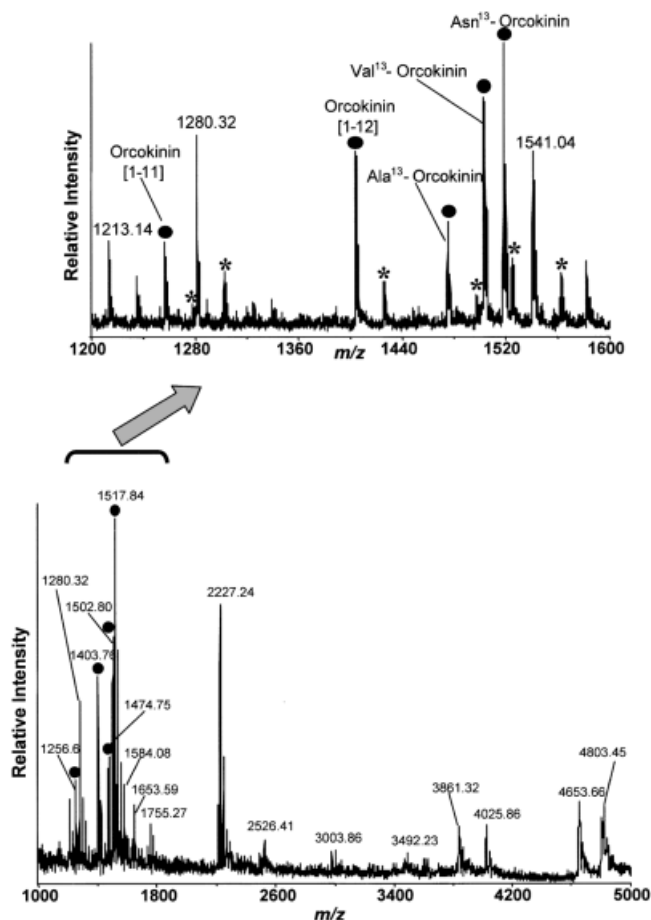


Fig. 11. Representative MALDI mass spectrum of a small piece of pericardial organ (PO) tissue from *H. americanus*. Signals generally correspond to protonated molecular ion, $[M + H]^+$, where M is the molecular weight of each peptide. Identified orcokinins are indicated with black dots and labeled in the expanded region of the spectrum. The asterisks indicate Na^+ adduct peaks.

0.04 in $[Ala^{13}]orcokinin$ ($P < 0.05$, $n = 5$). The onset of the PY neuron burst was earlier in $[Ala^{13}]orcokinin$ (phase of 0.72 ± 0.03 in normal saline and 0.60 ± 0.04 in $[Ala^{13}]orcokinin$, $P < 0.05$). The PY neuron burst offset and duty cycle were not significantly different in orcokinin. All of the effects of $[Ala^{13}]orcokinin$ were reversible (Fig. 15A) after washing for 15–30 minutes in normal saline.

DISCUSSION

Although it is now apparent that the nervous system contains a large number of neuropeptides (Hökfelt et al., 2000), we are far from having a complete description of the full complement of neuropeptides that modulate behaviorally relevant neural circuits. Additionally, we are only now beginning to have an appreciation of how neurons that contain multiple cotransmitters employ these, either singly or in concert, to modulate circuits in behavior (Nusbaum et al., 2001). The STG receives projections that contain a large number of neuropeptides (Marder et al., 1986, 1987; Nusbaum and Marder, 1988; Mortin and

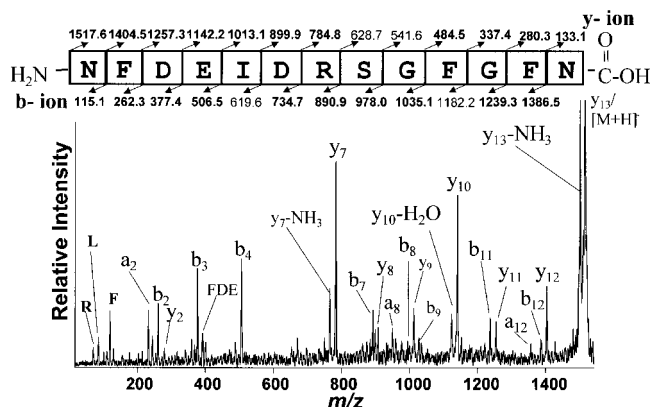


Fig. 12. MALDI-PSD sequencing of orcokinin from *H. americanus* brain extract. Shown at the top is the sequence analysis of orcokinin, with the N-terminal on the left and the C-terminal on the right. Single-letter amino acid abbreviations are used, N (Asn), F (Phe), D (Asp), E (Glu), I (Ile), R (Arg), S (Ser), and G (Gly). The observed b-type (bottom) and y-type (top) ion pairs are indicated by arrows. All the observed ions are shown in boldface. Below the sequence is the MALDI-PSD fragment ion spectrum of the precursor ion at m/z 1,517.6. N-terminal ion series such as a/b-ions and their loss of neutrals, C-terminal ion series such as y-ions, and several internal fragment ions as well as immonium ions are labeled in the spectrum.

Marder, 1991; Turrigiano and Selverston, 1991; Christie et al., 1994, 1997; Skiebe and Schneider, 1994). However, an eventual full understanding of the function of all of the modulatory projection neurons to the STG will require obtaining a relatively complete catalog of the potential cotransmitters in all these projection neurons. This paper describes the distribution of the orcokinins in the stomatogastric nervous system of three of the decapod species that are commonly used in electrophysiological studies of the neuromodulatory control of the central pattern generating circuits in the STG, *C. borealis*, *P. interruptus*, and *H. americanus*. This now adds the orcokinins to the list of substances likely to function as cotransmitters in identified modulatory projection neurons in the stomatogastric nervous system.

Biochemistry of the orcokinin peptides

The orcokinin peptides are neither N-terminally nor C-terminally blocked, which is atypical for most known invertebrate neuropeptides, though not without precedent (Keller, 1992). We found two C-terminally truncated forms of the original $[Asn^{13}]orcokinin$. Previous work (Bungart et al., 1995b) studying the bioactivity of orcokinin analogues in the hindgut assay showed that changes at the C-terminus interfere less with biological activity than changes at the N-terminus. Removal of more than one amino acid at the N-terminus resulted in a complete loss of activity, whereas the C-terminal deletion of three amino acids still produced an analogue with decreased affinity but physiological effectiveness. Bungart et al. (1995b) also found that C-terminal amidation did not cause loss of activity, suggesting that the C-terminal hydroxyl group does not seem to be important. Our electrophysiological results show that the STG has functional orcokinin receptors that respond to one of the orcokinins present in the neuropil. That said, it will be interesting to determine whether this receptor has properties similar to

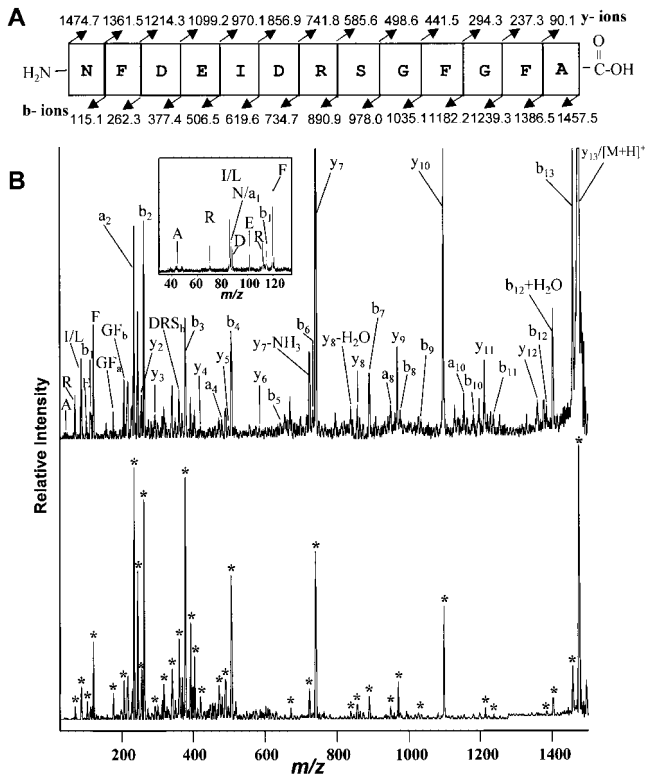


Fig. 13. MALDI-PSD analysis of the putative [Ala¹³]orcokinin peptide. **A:** Sequence of orcokinin, with the N-terminal on the left and the C-terminal on the right. Single-letter amino acid abbreviations are used, N (Asn), F (Phe), D (Asp), E (Glu), I (Ile), R (Arg), S (Ser), G (Gly), and A (Ala). The observed b-type (bottom) and y-type (top) ion pairs are indicated by arrows. **B:** MALDI-PSD fragment ion spectra of both the ion at *m/z* 1,474.6 from the LC fraction of brain extract from *C. borealis* (upper trace) and the synthetic orcokinin standard (lower trace). N-terminal ion series such as *a/b*-ions and their loss of neutrals, C-terminal ion series such as y-ions, and several internal fragment ions as well as immonium ions are labeled in the upper trace spectrum. The inset highlights the immonium ion region, with the amino acid residues labeled. The masses of the fragment ion signals labeled with asterisks in the lower trace are identical to fragment ions detected in the upper trace.

those described for crayfish hindgut. Moreover, it is certainly possible that there are multiple orcokinin receptors, expressed either by different target tissues in the animal or even within the same tissue.

Although we found a number of different orcokinin forms within each species, we saw no evidence that different analogues of this peptide family are found in different tissues. Thus far, the biochemical data (Table 1) show that multiple forms of the orcokinins are found in the same tissue, and there is a simple correspondence to the distribution seen immunocytochemically and that seen by direct biochemical investigation. Although the antibody we used was raised against [Asn¹³]orcokinin, the very close structural similarity of all of these forms makes it highly likely that the antibody will label all of the orcokinin forms that are detected biochemically. Therefore, MALDI data from different regions of the stomatogastric nervous system and various connecting nerves are important to determine the expression and distribution of various

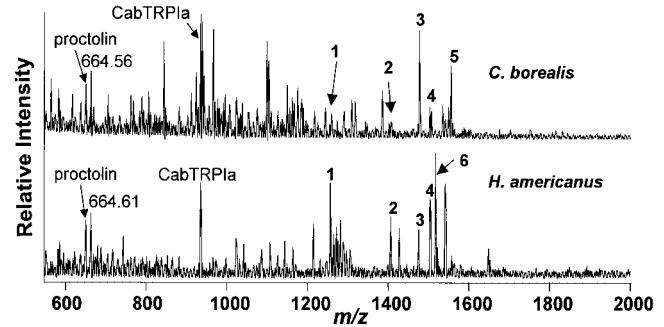
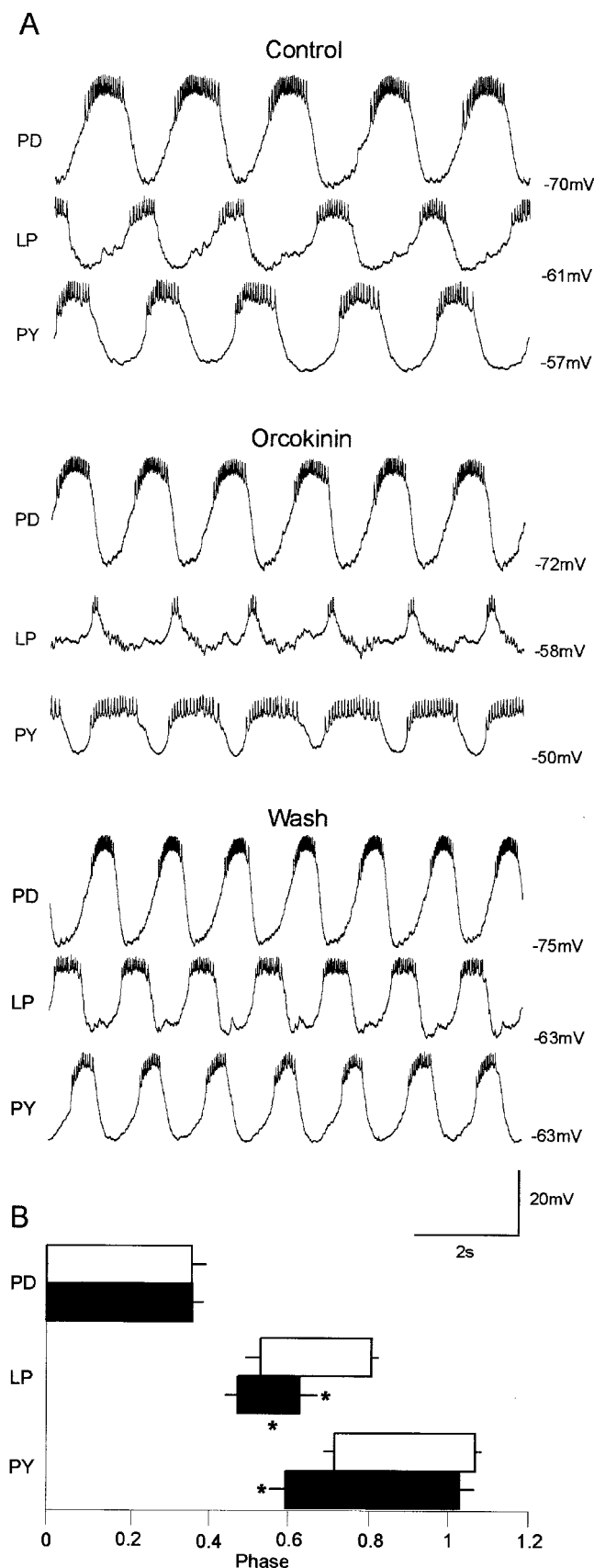


Fig. 14. MALDI-MS of small pieces of STG tissues from *C. borealis* (A) and *H. americanus* (B). Peaks labeled with numbers represent orcokinin peptides: 1, orcokinin[1–11]; 2, orcokinin[1–12]; 3, [Ala¹³]orcokinin; 4, [Val¹³]orcokinin; 5, [Ser⁹]orcokinin; 6, [Asn¹³]orcokinin.

forms of orcokinins. In fact, MALDI analyses of single identified orcokinin staining neurons, the PS cells, were performed to investigate whether individual neurons express multiple forms of the orcokinins (see discussion below). In *Procambarus clarkii*, there are two orcokinin genes, both of which encode the sequences for [Ala¹³]-, [Val¹³]-, [Asn¹³]-, and [Thr⁸-His¹³]orcokinins (Yasuda-Kamatani and Yasuda, 2000). This suggests that multiple forms of the orcokinins might be commonly expressed in individual neurons.

Orcokinins as cotransmitters in the PS/IV neurons

Dando and Selverston (1972) first characterized the physiological actions of a pair of neurons found in *P. interruptus* at the base of the brain (Claiborne and Selverston, 1984b) that project down the stn and significantly alter the motor patterns of the STG. In *P. interruptus*, these neurons contain histamine (Claiborne and Selverston, 1984a) and FLRFamide-like peptides (Kilman, 1998). In *C. borealis* the IV neuron somata are sometimes found in the ivn and also contain histamine and FLRFamide-like peptides (Christie, 1995; Christie et al., 2002). In *H. gammarus*, the IV neurons are called the pyloric suppressor (PS) neurons, have been extensively studied electrophysiologically (Cazalets et al., 1990a,b; Meyrand et al., 1991, 1994), and also contain histamine and FLRFamide peptides (Le Feuvre et al., 2001). In *H. americanus*, the PS/IV neurons contain histamine (Mulloney and Hall, 1991; Pulver et al., 2002). We show here with immunocytochemistry that in *H. americanus* these neurons also contain one or more of the orcokinins. By using MALDI-MS, peptide profiles from single isolated PS neurons from *H. americanus* were obtained. As shown in Table 1, three forms of orcokinins were detected, in addition to the detection of two extended FLRFamide peptides, SDRNFLRFamide and TNRNFLRFamide (data not shown). Thus the PS neurons of *H. americanus* contain histamine, extended FLRFamide peptides, and orcokinins. Orcokinin is also seen in the PS neurons in the freshwater crustacean *C. destructor* (Skiebe et al., 2002). Taken together, these data provide additional evidence for the orcokinins as cotransmitters in the PS/IV neurons. It will be interesting to determine in the future whether any of the physiological actions of the PS/IV neurons can be



attributed to the orcokinins and whether any of the physiological differences between the actions of the PS neurons in those species that contain orcokinins and those lacking these peptides can be attributed to the different cotransmitter complement in these animals.

Early appearance of the orcokinins in *H. americanus*

Some amine and peptide neuromodulators are present quite early in embryonic development, whereas others first appear late in larval life (Fénelon et al., 1998, 1999; Kilman et al., 1999; Le Feuvre et al., 2001). Moreover, some identified projection neurons acquire their cotransmitters at considerably different stages of development (Kilman et al., 1999; Le Feuvre et al., 2001). Here we show that the orcokinins are present in the embryonic stomatogastric nervous system and POs. Histamine immunoreactivity in the PS neurons is also present early in embryonic time in both *H. gammarus* (Le Feuvre et al., 2001) and *H. americanus* (Pulver et al., 2002). This suggests that the PS/IV neurons may acquire their full complement of cotransmitters early and that the PS neurons may play significant roles in the physiology of the embryonic and larval stomatogastric nervous system.

Comparative studies

To date orcokinins have been identified in a number of different crustacean species, including *P. clarkii* (Yasuda-Kamatani and Yasuda, 2000), *O. limosus* (Stangier et al., 1992), *C. maenas* (Bungart et al., 1995a), *C. destructor* (Skiebe et al., 2002), and now *C. borealis*, *H. americanus*, and *P. interruptus*. As shown in Table 2, the biochemical data demonstrate a considerable conservation of the orcoxinin forms, with [Ala¹³]-, [Val¹³]-, and [Asn¹³]orcokinins commonly found. Furthermore, based on MALDI mass profiling, it appears that another variant of orcoxinin, [Thr⁸-His¹³]orcoxinin, found in two crayfish species, namely, *P. clarkii* (Yasuda-Kamatani and Yasuda, 2000) and *C. destructor* (Skiebe et al., 2002), is present in *C. borealis*. In the four species in which the distribution of orcokinins has been studied throughout the stomatogastric nervous system, the main features of this distribution have been preserved (Figs. 5, 9). In at least two species there are projections from the PS neurons to the STG, and in all species there are somata in the OG and CoGs. However, as is the case with other neuropeptides (Mortin and Marder, 1991; Turrigiano and Selverston, 1991; Christie et al., 1995a), some aspects of the orcoxinin distribution showed species differences. For example, there are two stained neurons at the junction of the sons in *P. interruptus* and in *C. destructor* that we did not see in other species. These somata were seen with methylene blue stains but have not previously been found in immu-

Fig. 15. Physiological actions of orcoxinin on the pyloric rhythm of adult *H. americanus*. **A**: Each panel shows three simultaneous intracellular recordings from the PD, LP, and PY motor neurons. Top, control. Middle, in the presence of 2×10^{-6} M [Ala¹³]orcoxinin. Bottom, wash. **B**: Effects of orcoxinin on the phase relations of the pyloric motor pattern. Open bars, control; solid bars, in the presence of 2×10^{-6} M [Ala¹³]orcoxinin. Statistically significant changes ($P < 0.05$) are indicated by an asterisk placed at the beginning, end, or middle to indicate the phase of onset, phase of offset, and duty cycle, respectively. Pooled data from five experiments.

TABLE 2. Orcokinin Peptides Isolated From Crustaceans

| MW | Peptide ID | Peptide sequence ¹ | Species |
|---------|---|--|---|
| 1,188.2 | | Phe-Asp- Ala-Phe-Thr-Thr -Gly-Phe-Gly- His-Ser -OH | <i>P. clarkii</i> , ² <i>C. destructor</i> ³ |
| 1,256.5 | Orc[1–11] | Asn-Phe-Asp-Glu-Ile-Asp-Arg-Ser-Gly-Phe-Gly-OH | <i>H. americanus</i> , ⁴ <i>P. interruptus</i> , ⁴ <i>C. borealis</i> ⁴ |
| 1,403.6 | Orc[1–12] | Asn-Phe-Asp-Glu-Ile-Asp-Arg-Ser-Gly-Phe-Gly-Phe-OH | <i>H. americanus</i> , ⁴ <i>P. interruptus</i> , ⁴ <i>C. borealis</i> ⁴ |
| 1,458.7 | [Ala ⁸ -Ala ¹³]Orc | Asn-Phe-Asp-Glu-Ile-Asp-Arg- Ala -Gly-Phe-Gly-Phe- Ala -OH | <i>C. destructor</i> ³ |
| 1,474.6 | [Ala ¹³]Orc | Asn-Phe-Asp-Glu-Ile-Asp-Arg-Ser-Gly-Phe-Gly-Phe- Ala -OH | <i>C. maenas</i> , ⁵ <i>P. clarkii</i> , ² <i>C. borealis</i> , ⁴ <i>H. americanus</i> , ⁴ <i>P. interruptus</i> ⁴ |
| 1,502.7 | [Val ¹³]Orc | Asn-Phe-Asp-Glu-Ile-Asp-Arg-Ser-Gly-Phe-Gly-Phe- Val -OH | <i>O. limosus</i> , ⁶ <i>C. maenas</i> , ⁵ <i>P. clarkii</i> , ² <i>C. borealis</i> , ⁴ <i>H. americanus</i> , ⁴ <i>P. interruptus</i> , ⁴ <i>C. destructor</i> ³ |
| 1,517.7 | [Asn ¹³]Orc | Asn-Phe-Asp-Glu-Ile-Asp-Arg-Ser-Gly-Phe-Gly-Phe- Asn -OH | <i>O. limosus</i> , ⁶ <i>P. clarkii</i> , ² <i>H. americanus</i> , ⁴ <i>P. interruptus</i> , ⁴ <i>C. destructor</i> ³ |
| 1,547.7 | [Ser ⁹]Orc | Asn-Phe-Asp-Glu-Ile-Asp-Arg-Ser- Ser -Phe-Gly-Phe- Asn -OH | <i>C. maenas</i> , ⁵ <i>C. borealis</i> ⁴ |
| 1,554.6 | [Thr ⁸ -His ¹³]Orc | Asn-Phe-Asp-Glu-Ile-Asp-Arg- Thr -Gly-Phe-Gly-Phe- His -OH | <i>P. clarkii</i> , ² <i>C. destructor</i> , ³ <i>C. borealis</i> ⁴ |

¹Varied residues appear in boldface.

²Yasuda-Kamatani and Yasuda (2000) Gen Comp Endocrinol 118:161–172.

³Skiebe et al. (2001) J Comp Neurol (submitted).

⁴This paper.

⁵Bungart et al. (1995) Peptides 16:67–72.

⁶Bungart et al. (1994) Peptides 15:393–400.

nocytochemical studies of other modulators. Stained somata in the STG were seen in *C. borealis* and *C. destructor* (Skiebe et al., 2002) but not in the other species. In *C. destructor* one of the STG somata is the anterior median (AM) neuron (Skiebe et al., 2001), which innervates the intrinsic muscles of the cardiac sac. It will be interesting to determine whether the same is true in *C. borealis*.

The orcokinins are likely to function as both circulating hormones and local neuromodulators

The orcokinins are present both in the POs and in identified neurons that are known to modulate STG motor patterns. Thus the orcokinins can be added to the list of substances that can both have hormonal action and act as neurally released neurotransmitters/neuromodulators. In fact, there is a very extensive overlap between the substances that are found in the POs and in the descending pathways to the STG (Marder and Calabrese, 1996; Marder et al., 1997; Abbott and Marder, 1998). This means that the neuromodulatory environment under any set of physiological conditions can include a baseline concentration of hormonally released substance and synaptically liberated mixtures of cotransmitters. Therefore, orcokinin is likely always to be acting in concert with other neuromodulatory substances.

Physiological effects of orcokinin

In this study we demonstrate for the first time that the orcokinins can modulate the excitability of a central neural circuit. Interestingly, most of the neuropeptides found in descending projections to the STG, including the extended FLRFamides that colocalize with histamine and orcokinin in the PS neurons, excite the LP neuron (Weimann et al., 1993, 1997; Richards and Marder, 2000; Swensen, 2000; Swensen and Marder, 2000). In contrast, in the presence of orcokinin, the number of LP neuron spikes/burst decreased. Further work will be needed to determine the direct cellular targets of the orcokinins and the current(s) that they evoke or modulate. Nonetheless, the bias towards PY neuron activity seen in orcokinin makes it somewhat unusual among STG modulators. Of course, PS neuron activation is likely to deliver a complex mixture of orcokinin, histamine, and extended FLRFamides, so a great deal more remains to be understood about the potential roles each of these plays in the complex physiological changes evoked by PS neuron activation (Meyrand et al., 1992, 1994).

CONCLUSIONS

The widespread distribution of the orcokinins in the crustacean nervous system allows us to add them to the complement of neuromodulatory peptides, such as proctolin, the extended FLRFamides, and crustacean cardioactive peptide (CCAP), that all have profound physiological actions at many sites within the animal. Therefore, we anticipate that the orcokinins will play numerous and as yet poorly understood roles in many aspects of the control of complex behaviors.

ACKNOWLEDGMENTS

We thank Dr. Michael Tlusty of the New England Aquarium for supplying embryonic, larval, and juvenile *H. americanus* and Dr. Barbara Beltz and Wellesley College for the use of their confocal microscope. We thank Dr. Heinrich Dirksen for the kind gift of the orcokinin antibody and Dr. Petra Skiebe for sharing the results of her unpublished research with us. We also thank Dr. Dirk Bucher for assistance in image processing. This work was supported by National Institute of Neurological Disorder and Stroke grants NS17813 (E.M.) and NS31609 (J.V.S.).

LITERATURE CITED

- Abbott LF, Marder E. 1998. Modeling small networks. In: Koch C, Segev I, editors. Methods in neuronal modeling: from ions to networks. Cambridge, MA: MIT Press. p 361–410.
- Beltz BS, Kravitz EA. 1983. Mapping of serotonin-like immunoreactivity in the lobster nervous system. J Neurosci 3:585–602.
- Beltz B, Eisen JS, Flamm R, Harris-Warrick RM, Hooper S, Marder E. 1984. Serotonergic innervation and modulation of the stomatogastric ganglion of three decapod crustaceans (*Panurilus interruptus*, *H. americanus* and *Cancer irroratus*). J Exp Biol 109:35–54.
- Bungart D, Dirksen H, Keller R. 1994. Quantitative determination and distribution of the myotropic neuropeptide orcokinin in the nervous system of astacidean crustaceans. Peptides 15:393–400.
- Bungart D, Hilbich C, Dirksen H, Keller R. 1995a. Occurrence of analogues of the myotropic neuropeptide orcokinin in the shore crab, *Carcinus maenas*: evidence for a novel neuropeptide family. Peptides 16:67–72.
- Bungart D, Kegel G, Burdzik S, Keller R. 1995b. Structure–activity relationships of the crustacean myotropic neuropeptide orcokinin. Peptides 16:199–204.
- Cazalets J, Nagy F, Moulins M. 1990a. Suppressive control of the crustacean pyloric network by an identified neuron. I. Modulation of the motor pattern. J Neurosci 10:448–457.
- Cazalets JR, Nagy F, Moulins M. 1990b. Suppressive control of the crustacean pyloric network by a pair of identified interneurons. II. Modulation of neuronal properties. J Neurosci 10:458–468.

- Christie A. 1995. Chemical neuroanatomy of the crab stomatogastric ganglion: a study using immunocytochemistry and laser scanning confocal microscopy. PhD thesis, Department of Biology, Brandeis University. p 156.
- Christie AE, Hall C, Oshinsky M, Marder E. 1994. Buccalin-like and myomodulin-like peptides in the stomatogastric ganglion of the crab *Cancer borealis*. *J Exp Biol* 193:337–343.
- Christie AE, Baldwin D, Turrigiano G, Graubard K, Marder E. 1995a. Immunocytochemical localization of multiple cholecystokinin-like peptides in the stomatogastric nervous system of the crab, *Cancer borealis*. *J Exp Biol* 198:263–271.
- Christie AE, Skiebe P, Marder E. 1995b. Matrix of neuromodulators in neurosecretory structures of the crab, *Cancer borealis*. *J Exp Biol* 198:2431–2439.
- Christie AE, Lundquist T, Nässel DR, Nusbaum MP. 1997. Two novel tachykinin-related peptides from the nervous system of the crab *Cancer borealis*. *J Exp Biol* 200:2279–2294.
- Christie AE, Stein W, Quinlan JE, Beenhakker MP, Marder E, Nusbaum MP. 2002. Actions of a histaminergic/peptidergic projection neuron on rhythmic motor patterns in the stomatogastric nervous system of the crab *Cancer borealis*. In preparation.
- Claiborne B, Selverston A. 1984a. Histamine as a neurotransmitter in the stomatogastric nervous system of the spiny lobster. *J Neurosci* 4:708–721.
- Claiborne B, Selverston A. 1984b. Localization of stomatogastric IV neuron cell bodies in the lobster brain. *J Comp Physiol* 154:27–32.
- Cooke IM, Sullivan RE. 1982. Hormones and neurosecretion. In: Atwood HL, Sandeman DC, editors. *The biology of Crustacea: neurobiology*. New York: Academic Press. p 205–290.
- Dando MR, Selverston AI. 1972. Command fibres from the supraoesophageal ganglion to the stomatogastric ganglion in *Panulirus argus*. *J Comp Physiol* 78:138–175.
- Dircksen H. 1997. Conserved crustacean cardioactive peptide: neural networks and function in arthropod evolution. In: Coast GM, Webster SG, editors. *Arthropod endocrinology—perspectives and recent advances*. Cambridge: Cambridge University Press.
- Dircksen H, Burdzik S, Sauter A, Keller R. 2000. Two orcokinins and the novel octapeptide orcomyotropin in the hindgut of the crayfish *Orconectes limosus*: identified myostimulatory neuropeptides originating together in neurones of the terminal abdominal ganglion. *J Exp Biol* 203:2807–2818.
- Fénelon V, Casasnovas B, Faumont S, Meyrand P. 1998. Ontogenetic alteration in peptidergic expression within a stable neuronal population in lobster stomatogastric nervous system. *J Comp Neurol* 399:289–305.
- Fénelon VS, Kilman V, Meyrand P, Marder E. 1999. Sequential developmental acquisition of neuromodulatory inputs to a central pattern-generating network. *J Comp Neurol* 408:335–351.
- Floyd PD, Li L, Moroz TP, Sweedler JV. 1999. Characterization of peptides from *Aplysia* using microbore liquid chromatography with matrix-assisted laser desorption/ionization time-of-flight mass spectrometry guided purification. *J Chromatol A* 830:105–113.
- Garden RW, Moroz LL, Moroz TP, Shippy SA, Sweedler JV. 1996. Excess salt removal with matrix rinsing: direct peptide profiling of neurons from marine invertebrates using matrix-assisted laser desorption/ionization time-of-flight mass spectrometry. *J Mass Spectrom* 31:1126–1130.
- Garden RW, Shippy SA, Li L, Moroz TP, Sweedler JV. 1998. Proteolytic processing of the *Aplysia* egg-laying hormone prohormone. *Proc Natl Acad Sci USA* 95:3972–3977.
- Harris-Warrick RM, Marder E, Selverston AI, Moulins M. 1992. *Dynamic biological networks. The stomatogastric nervous system*. Cambridge, MA: MIT Press.
- Helluy SM, Beltz BS. 1991. Embryonic development of the American lobster: quantitative staging and characterization of an embryonic molt cycle. *Biol Bull* 180:355–371.
- Hökfelt T, Broberger C, Xu ZQ, Sergejev V, Ubink R, Diez M. 2000. Neuropeptides—an overview. *Neuropharmacology* 39:1337–1356.
- Jiménez CR, van Veelen PA, Li KW, Wildering WC, Geraerts WPM, Tjaden UR, van der Greef J. 1994. Neuropeptide expression and processing as revealed by direct matrix-assisted laser desorption ionization mass spectrometry of single neurons. *J Neurochem* 62:404–409.
- Keller R. 1992. Crustacean neuropeptides: structures, functions and comparative aspects. *Experientia* 48:439–448.
- Kilman VL. 1998. Multiple roles of neuromodulators throughout life: an anatomical study of the crustacean stomatogastric nervous system. PhD thesis, Neuroscience Program, Brandeis University. p 173.
- Kilman VL, Fénelon V, Richards KS, Thirumalai V, Meyrand P, Marder E. 1999. Sequential developmental acquisition of cotransmitters in identified sensory neurons of the stomatogastric nervous system of the lobsters, *Homarus americanus* and *Homarus gammarus*. *J Comp Neurol* 408:318–334.
- Le Feuvre Y, Fénelon VS, Meyrand P. 2001. Ontogeny of modulatory inputs to motor networks: early established projection and progressive neurotransmitter acquisition. *J Neurosci* 21:1313–1326.
- Li L, Garden RW, Romanova EV, Sweedler JV. 1999. In situ sequencing of peptides from biological tissues and single cells using MALDI-PSD/CID analysis. *Anal Chem* 71:5451–5458.
- Li L, Pulver S, Kelley WP, Sweedler JV, Marder E. 2001. Comparative studies of the orcokinins peptides in crustacean species by immunocytochemistry and mass spectrometry. *Soc Neurosci Abstr* 27:909.1.
- Marder E, Calabrese RL. 1996. Principles of rhythmic motor pattern generation. *Physiol Rev* 76:687–717.
- Marder E, Hooper SL, Siwicki KK. 1986. Modulatory action and distribution of the neuropeptide proctolin in the crustacean stomatogastric nervous system. *J Comp Neurol* 243:454–467.
- Marder E, Calabrese RL, Nusbaum MP, Trimmer B. 1987. Distribution and partial characterization of FMRFamide-like peptides in the stomatogastric nervous systems of the rock crab, *Cancer borealis*, and the spiny lobster, *Panulirus interruptus*. *J Comp Neurol* 259:150–163.
- Marder E, Christie AE, Kilman VL. 1995. Functional organization of cotransmission systems: lessons from small nervous systems. *Invert Neurosci* 1:105–112.
- Marder E, Jorge-Rivera JC, Kilman V, Weimann JM. 1997. Peptidergic modulation of synaptic transmission in a rhythmic motor system. In: Festoff BW, Hantai D, Citron BA, editors. *Advances in organ biology*. Greenwich, CT: JAI Press Inc. p 213–233.
- Martin G, Sorokine O, Moniatte M, Juchault P, Van Dorsselaer A. 1999. Profiling the peptides in two neurohemal organs, the sinus gland and lateral nervous plexus of terrestrial isopods (Crustacea), by mass spectrometry. *Can J Zool* 77:1300–1308.
- Meyrand P, Simmers J, Moulins M. 1991. Construction of a pattern-generating circuit with neurons of different networks. *Nature* 351:60–63.
- Meyrand P, Weimann JM, Marder E. 1992. Multiple axonal spike initiation zones in a motor neuron: serotonin activation. *J Neurosci* 12:2803–2812.
- Meyrand P, Simmers J, Moulins M. 1994. Dynamic construction of a neural network from multiple pattern generators in the lobster stomatogastric nervous system. *J Neurosci* 14:630–644.
- Meyrand P, Faumont S, Simmers J, Christie AE, Nusbaum MP. 2000. Species-specific modulation of pattern-generating circuits. *Eur J Neurosci* 12:2585–2596.
- Mortin LI, Marder E. 1991. Differential distribution of β -pigment dispersing hormone (β -PDH)-like immunoreactivity in the stomatogastric nervous system of five species of decapod crustaceans. *Cell Tissue Res* 265:19–33.
- Mulloney B, Hall WM. 1991. Neurons with histaminelike immunoreactivity in the segmental and stomatogastric nervous systems of the crayfish *Pacifastacus leniusculus* and the lobster *Homarus americanus*. *Cell Tissue Res* 266:197–207.
- Nusbaum MP, Marder E. 1988. A neuronal role for a crustacean red pigment concentrating hormone-like peptide: neuromodulation of the pyloric rhythm in the crab, *Cancer borealis*. *J Exp Biol* 135:165–181.
- Nusbaum MP, Blitz DM, Swensen AM, Wood D, Marder E. 2001. The roles of co-transmission in neural network modulation. *Trends Neurosci* 24:146–154.
- Pulver SR, Thirumalai V, Richards KS, Marder E. 2002. The distribution and actions of histamine in the adult and developing stomatogastric nervous system of the lobster, *Homarus americanus*. In preparation.
- Richards KS, Marder E. 2000. The actions of crustacean cardioactive peptide on adult and developing stomatogastric ganglion motor patterns. *J Neurobiol* 44:31–44.
- Siuzdak G. 1996. Sequencing of peptides and proteins. In: Siuzdak G, editor. *Mass spectrometry for biotechnology*. San Diego: Academic Press. p 93–99.
- Skiebe P. 1999. Allatostatin-like immunoreactivity within the stomatogastric nervous system and the pericardial organs of the crab *Cancer pagurus*, the lobster *Homarus americanus*, and the crayfish *Cherax destructor* and *Procambarus clarkii*. *J Comp Neurol* 403:85–105.

- Skiebe P, Ganeshina O. 2000. Synaptic neuropil in nerves of the crustacean stomatogastric nervous system: an immunocytochemical and electron microscopical study. *J Comp Neurol* 420:373–397.
- Skiebe P, Schneider H. 1994. Allatostatin peptides in the crab stomatogastric nervous system: inhibition of the pyloric motor pattern and distribution of allatostatin-like immunoreactivity. *J Exp Biol* 194:195–208.
- Skiebe P, Dreger M, Meseke M, Evers JF, Hucho F. 2002. Identification of orcokinin in single neurons in the stomatogastric nervous system of the crayfish, *Cherax destructor*. *J Comp Neurol* 444:245–259.
- Spengler B. 1997. Post-source decay analysis in matrix-assisted laser desorption/ionization mass spectrometry of biomolecules. *J Mass Spectrom*. 32:1019–1036.
- Stangier J, Hilbich C, Burdzik S, Keller R. 1992. Orcokinin: a novel myotropic peptide from the nervous system of the crayfish, *Orconectes limosus*. *Peptides* 13:859–864.
- Stefanini M, De Martino C, Zamboni L. 1967. Fixation of ejaculated spermatozoa for electron microscopy. *Nature* 216:173–174.
- Swensen AM. 2000. Network consequences of convergent modulation in the stomatogastric nervous system of the crab, *Cancer borealis*. Thesis, Neuroscience Program, Brandeis University. p 143.
- Swensen AM, Marder E. 2000. Multiple peptides converge to activate the same voltage-dependent current in a central pattern-generating circuit. *J Neurosci* 20:6752–6759.
- Turrigiano GG, Selverston AI. 1991. Distribution of cholecystokinin-like immunoreactivity within the stomatogastric nervous systems of four species of decapod crustacea. *J Comp Neurol* 305:164–176.
- Weimann JM, Marder E, Evans B, Calabrese RL. 1993. The effects of SDRN-FLRFamide and TNRNFLRFamide on the motor patterns of the stomatogastric ganglion of the crab *Cancer borealis*. *J Exp Biol* 181:1–26.
- Weimann JM, Skiebe P, Heinzel H-G, Soto C, Kopell N, Jorge-Rivera JC, Marder E. 1997. Modulation of oscillator interactions in the crab stomatogastric ganglion by crustacean cardioactive peptide. *J Neurosci* 17:1748–1760.
- Yasuda-Kamatani Y, Yasuda A. 2000. Identification of orcokinin gene-related peptides in the brain of the crayfish *Procambarus clarkii* by the combination of MALDI-TOF and on-line capillary HPLC/Q-ToF mass spectrometry and molecular cloning. *Gen Comp Endocrinol* 118:161–172.